



<b>Publication Year</b>	2019
<b>Acceptance in OA</b>	2020-12-30T11:17:11Z
<b>Title</b>	Relativistic Jets in Gamma-Ray-Emitting Narrow-Line Seyfert 1 Galaxies
<b>Authors</b>	D'AMMANDO, FILIPPO
<b>Publisher's version (DOI)</b>	10.3390/galaxies7040087
<b>Handle</b>	<a href="http://hdl.handle.net/20.500.12386/29355">http://hdl.handle.net/20.500.12386/29355</a>
<b>Journal</b>	GALAXIES
<b>Volume</b>	7

Review

# Relativistic Jets in Gamma-Ray-Emitting Narrow-Line Seyfert 1 Galaxies

Filippo D'Ammando

INAF—Istituto di Radioastronomia, Via P. Gobetti 101, I-40129 Bologna, Italy; dammando@ira.inaf.it

Received: 8 September 2019; Accepted: 4 November 2019; Published: date

**Abstract:** Before the launch of the *Fermi Gamma-ray Space Telescope* satellite only two classes of active galactic nuclei (AGN) were known to generate relativistic jets and thus to emit up to the  $\gamma$ -ray energy range: blazars and radio galaxies, both hosted in giant elliptical galaxies. The discovery by the Large Area Telescope (LAT) on-board the *Fermi* satellite of variable  $\gamma$ -ray emission from a few radio-loud narrow-line Seyfert 1 galaxies (NLSy1) revealed the presence of an emerging third class of AGN with powerful relativistic jets. Considering that NLSy1 are usually hosted in late-type galaxies with relatively small black hole masses, this finding opened new challenging questions about the nature of these objects, the disc/jet connection, the emission mechanisms at high energies, and the formation of relativistic jets. In this review, I will discuss the broad-band properties of the  $\gamma$ -ray-emitting NLSy1 included in the Fourth *Fermi* LAT source catalog, highlighting major findings and open questions regarding jet physics, black hole mass estimation, host galaxy and accretion process of these sources in the *Fermi* era.

**Keywords:** relativistic jet; gamma-rays; X-rays; optical; radio; emission mechanism; Seyfert galaxy; super-massive black hole; host galaxy

## 1. Introduction

Only a small percentage of active galactic nuclei (AGN) is radio-loud, and this characteristic is commonly ascribed to the presence of a relativistic jet, roughly perpendicular to the accretion disc. Relativistic jets are the most extreme manifestation of the power that can be generated by a super-massive black hole (SMBH) in the center of an AGN. Their emission is observed across the entire electromagnetic spectrum with a large fraction of the power emitted in  $\gamma$ -rays. Before the launch of the *Fermi Gamma-ray Space Telescope* satellite only two classes of AGN were known to generate strong relativistic jets, therefore to emit up to the  $\gamma$ -ray energy range: blazars and radio galaxies [1], both hosted in giant elliptical galaxies [2]. The observations by the Large Area Telescope (LAT) on board the *Fermi* satellite confirmed that the extragalactic  $\gamma$ -ray sky is dominated by blazars, with only a few radio galaxies detected [3,4]. However, the discovery by *Fermi*-LAT of variable  $\gamma$ -ray emission from a few radio-loud narrow-line Seyfert 1 galaxies (NLSy1) revealed the presence of a possible third class of AGN with powerful relativistic jets<sup>1</sup> (e.g., [6–8]).

NLSy1 represent a rare type of Seyfert galaxies identified by [9] and characterized by their optical properties: narrow permitted emission lines (full width at half maximum, FWHM ( $H\beta$ )  $< 2000 \text{ km s}^{-1}$ ), weak [OIII]/ $\lambda 5007$  emission lines (i.e., [OIII]/ $H\beta < 3$ ), and usually strong Fe II emission complexes

<sup>1</sup> Based on the new classification proposed by [5], these sources can be defined as “jetted AGN”.

(e.g., [10,11]). In X-rays they exhibit strong and rapid variability, steep spectra, relatively high luminosity, and substantial soft X-ray excess below 2 keV (e.g., [12–14]). These observational characteristics point to systems with smaller masses of the central SMBH ( $10^6$ – $10^8 M_{\odot}$ ) and higher Eddington ratios (close to or above the Eddington limit) with respect to blazars and radio galaxies (e.g., [15–17]). Optical estimates of BH mass suggested that NLSy1 lies below the  $M_{BH}$ – $\sigma_{bulge}$  relation, where  $\sigma_{bulge}$  is the velocity dispersion of the galaxy bulge (e.g., [18,19]). This suggested that NLSy1 are accreting at very high rate (e.g., [20]) and are objects in the early stages of their evolution (e.g., [21]). However, the use of optical methods to determine the BH mass of NLSy1 has been challenged by several authors. In fact, the effects of radiation pressure on the broad line region (BLR) clouds should be higher in case of highly accreting AGN, leading to underestimated masses [22]. In the same way, in case of a disc-like geometry of the BLR, projection effects could explain the smaller masses estimated in NLSy1 [23]. Fitting the optical spectrum of a large sample of NLSy1, [24] found a mean BH mass of  $\sim 10^8 M_{\odot}$  for both radio-quiet and radio-loud NLSy1 similar to the values obtained for broad-line Seyfert galaxies. The masses derived by the accretion disc model are one order of magnitude larger than their virial estimates. Virial estimates are prone to large uncertainties (e.g., [25]), suggesting that values obtained by fitting the accretion disc model, independent of the geometry and the kinematics of the BLR, should be more realistic (e.g., [26]).

The huge spectroscopic database of the Sloan Digital Sky Survey (SDSS; [27]) enables the selection of large NLSy1 samples (e.g., [15–17]). NLSy1 are generally radio-quiet (radio-loudness  $R$  being defined here as ratio of rest-frame 1.4 GHz and 4400 Å flux densities,  $R > 10$ ), with only a small fraction ( $< 7\%$ ; [15,17,28,29]) classified as radio-loud, while  $\sim 15\%$  of quasars are radio-loud (e.g., [30]). NLSy1 with higher values of radio-loudness ( $R > 100$ ) are even more sparse ( $\sim 3\%$ ). Radio-loud NLSy1 usually show a compact morphology with a core-jet structure extending up to a few parsec, with some cases in which the radio emission extends on kpc scales [31–35]. Together with high values of brightness temperature and core dominance this suggested the presence of a relativistic jet (e.g., [36]). In the past several authors have investigated the peculiarities of radio-loud NLSy1 with non-simultaneous radio-to-X-ray data, suggesting similarities with the young stage of quasars or different types of blazars (e.g., [16,29,37]). The detection of a few radio-loud NLSy1 in  $\gamma$ -rays by *Fermi*-LAT has been an unchallengeable evidence of the presence of highly relativistic jets in this class of AGN. In addition, apparent superluminal jet components were observed in SBS 0846+513 [38], PMN J0948+0022 and 1H 0323+342 [39], suggesting high ( $>10$ ) Lorentz factors and small ( $<10^\circ$ ) viewing angles.

NLSy1 are usually hosted in spiral galaxies (e.g., [40–44]), although some objects are associated with early type S0 galaxies (e.g., Mrk 705 and Mrk 1239; [45]). The presence of a relativistic jet in these sources seems to be in contrast to the paradigm that powerful jets could be produced only in elliptical galaxies (e.g., [46,47]). Indeed, the most powerful jets are found in luminous elliptical galaxies with very massive ( $10^8$ – $10^{10} M_{\odot}$ ) SMBH (e.g., [48]). This is interpreted as indirect evidence that a high spin is required for the jet production. In fact, elliptical galaxies should be the result of a major merger event that is required for spinning up the central BH (e.g., [49]). The detection of variable  $\gamma$ -ray emission from radio-loud NLSy1 poses intriguing questions about the nature of these sources, the production of relativistic jets, and the mechanisms of high-energy emission in the different class of AGN. In this context the study of NLSy1 has received increasing attention.

Nine NLSy1 are included in the recent Fourth *Fermi* LAT source catalog (4FGL, [3]), which covers 8 years (i.e., 4 August 2008–2 August 2016) of LAT data in the energy range from 50 MeV to 1 TeV. In this paper I will review the radio-to- $\gamma$ -ray properties of the  $\gamma$ -ray-emitting sources present in the 4FGL catalog and classified as bona-fide NLSy1. Although biased by the author’s scientific interests, a balanced review of relevant works on the selected topics is attempted. The paper is organized as follows. The  $\gamma$ -ray properties of NLSy1 are discussed in Section 2, while Sections 3–5 are devoted to the X-ray, infrared-optical, and radio properties of the  $\gamma$ -ray-emitting NLSy1, respectively. Results about

the spectral energy distribution (SED) modelling of these sources are reported in Section 6, while their BH mass and host galaxy are discussed in Section 7. Finally, I draw some conclusions in Section 8. Throughout the paper, a  $\Lambda$  cold dark matter cosmology with  $H_0 = 67 \text{ km s}^{-1} \text{ Mpc}^{-1}$ ,  $\Omega_\Lambda = 0.68$  and  $\Omega_m = 0.32$  [50] is adopted.

## 2. The $\gamma$ -ray Properties

Four radio-loud NLSy1 galaxies have been detected at high significance by *Fermi*-LAT in the first year of operation (i.e., 1H 0323+342, PMN J0948+0022, PKS 1502+036, and PKS 2004–447<sup>2</sup>) and are included in the First *Fermi* LAT source catalog, based on the first 11 months of LAT operation (1FGL; [54]). No new  $\gamma$ -ray emitting NLSy1 has been reported in the Second *Fermi* LAT source catalog, including observations performed between 4 August 2008 and 31 July 2010 (2FGL; [55]), with respect to the 1FGL catalog. SBS 0846+513 was detected in  $\gamma$ -rays for the first time during October 2010–August 2011, when a significant increase of activity was observed by LAT [56]. Thus in the Third *Fermi* LAT source catalog (3FGL), based on the first 4 years of LAT operation, five NLSy1 have been reported [4]. The first  $\gamma$ -ray detection of FBQS J1644+2619 has been reported in [57], analysing the  $\gamma$ -ray data collected on a longer period than that of 3FGL, i.e., August 2008–December 2014. Both the LAT detection of high  $\gamma$ -ray activity periods from FBQS J1644+2619 observed from November 2008 to January 2009 and July to October 2012 correspond to periods of high optical activity, as observed in *V*-band by the Catalina Real-Time Transient survey. That has confirmed the association of the  $\gamma$ -ray source with the NLSy1 FBQS J1644+2619. With the new Pass 8 event-level analysis (e.g., [58]) and by using 7 and 8.5 years of *Fermi*-LAT data other two new NLSy1 have been detected for the first time in  $\gamma$ -rays, B3 1441+476 and TXS 2116–077, as reported in [6,59], respectively. Another  $\gamma$ -ray-emitting NLSy1 has been included in the Fourth *Fermi* LAT source catalog (4FGL, [3]), IERS B1303+515, for a total of nine NLSy1 reported in the 4FGL catalog.

The  $\gamma$ -ray properties of the radio-loud NLSy1 included in the 4FGL catalog are reported in Table 1. The nine NLSy1 detected at high significance by *Fermi*-LAT up to now span a redshift range between 0.061 and 0.787. Luminosity, variability and spectral properties of the NLSy1 in  $\gamma$ -rays indicate a blazar-like behaviour (e.g., [6,59]). The average apparent  $\gamma$ -ray isotropic luminosity of these sources in the 0.1–300 GeV energy band is between  $2 \times 10^{44}$  and  $8 \times 10^{46} \text{ erg s}^{-1}$ , a range of values typical of blazars, in particular of FSRQ. This is an indication of a relatively small viewing angle with respect to the jet axis for these NLSy1, and therefore a high beaming factor for their  $\gamma$ -ray emission, similarly to what is inferred for FSRQ.

---

<sup>2</sup> PKS 2004–447 has a weak Fe II emission line with respect to the typical NLSy1 (for a discussion about the nature of this source see e.g., [51–53]).

**Table 1.** The  $\gamma$ -ray properties of radio-loud NLSy1 detected by *Fermi*-LAT. Energy flux and spectral parameters are taken from the 4FGL catalog [3].

Source Name	Redshift $z$	Energy Flux ( $E > 0.1$ GeV) $\times 10^{-11}$ erg cm $^{-2}$ s $^{-1}$	$\Gamma_\gamma$	$\alpha$	$\beta$	$L_\gamma$ erg s $^{-1}$
1H 0323+342	0.061	$2.17 \pm 0.10$	$2.82 \pm 0.04$	$2.72 \pm 0.05$	$0.10 \pm 0.03$	$2.1 \times 10^{44}$
SBS 0846+513	0.584	$2.17 \pm 0.08$	$2.17 \pm 0.02$	$2.27 \pm 0.04$	$0.08 \pm 0.02$	$3.2 \times 10^{46}$
PMN J0948+0022	0.585	$5.00 \pm 0.10$	$2.64 \pm 0.02$	$2.46 \pm 0.03$	$0.16 \pm 0.02$	$7.5 \times 10^{46}$
IERS B1303+515	0.787	$0.22 \pm 0.04$	$2.85 \pm 0.17$	–	–	$6.9 \times 10^{45}$
B3 1441+476	0.705	$0.20 \pm 0.04$	$2.56 \pm 0.11$	$2.25 \pm 0.26$	$0.41 \pm 0.19$	$4.7 \times 10^{45}$
PKS 1502+036	0.408	$1.61 \pm 0.08$	$2.59 \pm 0.04$	$2.48 \pm 0.06$	$0.10 \pm 0.03$	$1.0 \times 10^{46}$
FBQS J1644+2619	0.145	$0.45 \pm 0.06$	$2.78 \pm 0.10$	–	–	$2.7 \times 10^{44}$
PKS 2004–447	0.240	$0.92 \pm 0.08$	$2.60 \pm 0.05$	$2.41 \pm 0.09$	$0.18 \pm 0.06$	$1.7 \times 10^{45}$
TXS 2116–077	0.260	$0.32 \pm 0.06$	$2.83 \pm 0.15$	–	–	$7.2 \times 10^{44}$

In the same way, the average photon index  $\Gamma_\gamma$  of the  $\gamma$ -ray-emitting NLSy1 ranges between 2.2 and 2.9, a range of values usually observed in FSRQ [3,60]. For six of the nine sources the  $\gamma$ -ray spectrum is significantly curved ( $TS_{curv} > 9^3$ ), and a log-parabola model is preferred over a simple power-law model. In that case the spectral slope ( $\alpha$ ) and curvature parameter ( $\beta$ ) have been reported in Table 1, together with the photon index obtained with the power-law model. A significant spectral curvature is usually observed in the  $\gamma$ -ray spectra of FSRQ, suggesting similarities in the physical processes at work in these two classes of  $\gamma$ -ray-emitting AGN. The jet powers of  $\gamma$ -ray-emitting NLSy1 (obtained by the SED modelling) are similar to the values obtained for low-synchrotron-peaked BL Lacs and at the low end of the FSRQ distribution (e.g., [38,61,63–65]). However, the jet power depends on the BH mass, therefore the use of an underestimated BH mass value (see Section 7) leads to an underestimated jet power. After correcting for higher SMBH values, the jet powers of  $\gamma$ -ray-emitting NLSy1 should be comparable to those usually obtained for FSRQ.

Some of the  $\gamma$ -ray-emitting NLSy1 do exhibit large-amplitude  $\gamma$ -ray flares: SBS 0846+513 [38,56] (see Figure 1, left panel); PMN J0948+0022 [61,62] (see Figure 2, left panel), 1H 0323+342 [65], PKS 1502+036 [63], PKS 2004–447 [66], with an apparent isotropic  $\gamma$ -ray luminosity of  $\sim 10^{48}$  erg s $^{-1}$ , comparable to that of bright FSRQ. This is another indication that NLSy1 are able to host relativistic jets as powerful as those in FSRQ. Variability was observed during all  $\gamma$ -ray flares on a daily time-scale, and a subdaily time-scale in case of PKS 1502+036 [63,67] (see Figure 1, right panel). The  $\gamma$ -ray flaring activity of SBS 0846+513 and PMN J0948+0022 has been associated with a moderate spectral evolution, a behaviour observed also in bright FSRQ and low-synchrotron-peaked BL Lacs (e.g., [68]).

<sup>3</sup>  $TS_{curv} = 2 \log(\text{Likelihood}(\log\text{-parabola})/\text{Likelihood}(\text{power-law}))$ , i.e., a comparison of the likelihood function changing only the spectral representation of the source.

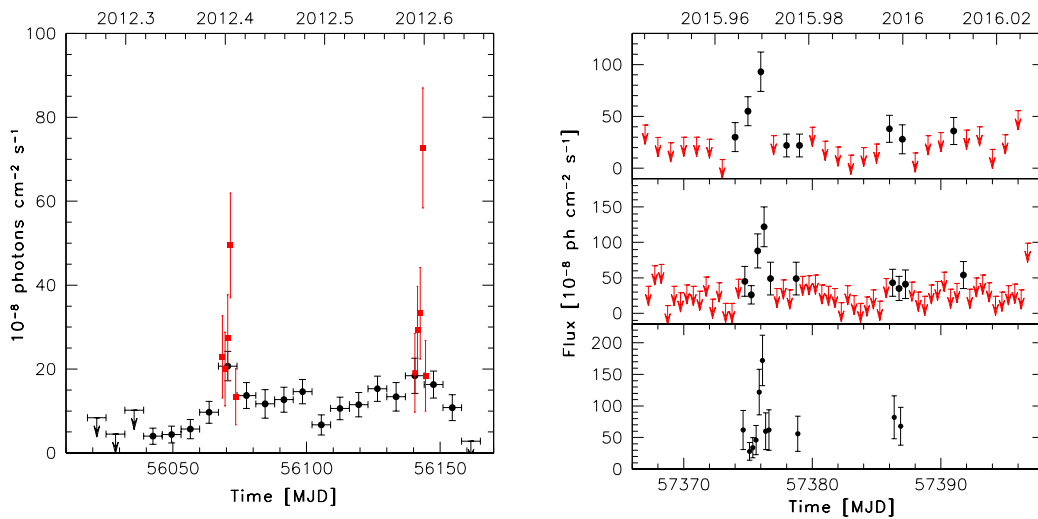


**Figure 1.** *Left panel:* LAT light curve of SBS 0846+513 in the 0.1–100 GeV energy range during 1 April–28 August 2012 with 7 days or 1 day (shown as red squares) time bins. Adapted from [38]. *Right panel:* LAT light curve of PKS 1502+036 in the 0.1–300 GeV energy range during 11 December 2015–9 January 2016, with 1-d time bins (top panel), 12-h time bins (middle panel), and 6-h time bins (bottom panel). Adapted from [63]. In both panels arrow refers to  $2\text{-}\sigma$  upper limits. Upper limits are computed when  $TS < 10$ .

In addition to the nine NLSy1 reported in the 4FGL catalogue, the  $\gamma$ -ray detection of other NLSy1 has been claimed in literature: FBQS J1102+2239 [64], FBQS J0956+2515 [69], NVSS J142106+385522 [59], and SDSS J164100.10+345452.7 [70]. However, these sources are not included in any LAT catalogue and their detection is not confirmed by dedicated analysis (e.g., [6]). Moreover, SDSS J003159.85+093618.4 has been proposed as counterpart of the unidentified  $\gamma$ -ray source 3FGL J0031.6+0938 and classified as a NLSy1 [71], but the  $\gamma$ -ray source is not confirmed in the 4FGL catalogue. In addition, some confirmed  $\gamma$ -ray sources already present in the 3FGL catalogue has been tentatively classified as NLSy1 in [59]: 3FGL J0937.7+5008 (corresponding to GB6 J0937+5008), 3FGL J1520.3+4209 (corresponding to B3 1518+423), and 3FGL J2118.4+0013 (corresponding to PMN J2118+0013), based on the NLSy1 catalog prepared by [15]. However, in that catalog less restrictive criteria has been used to classify a source as a NLSy1 (i.e.,  $\text{FWHM}(\text{H}\beta) < 2200 \text{ km s}^{-1}$  and a strong Fe bump not needed) with respect to the historical ones. Although no sharp change occurred at FWHM values equal to  $2000 \text{ km s}^{-1}$ , AGN properties change as a function of broad-line width, suggesting to keep a more conservative threshold as selection criterion. Moreover, in some cases the determination of the FWHM of the emission line depends on the assumed line shape (Gaussian or Lorentzian) and the contribution of the narrow line component to the total line flux, as in the case of 4C +04.42 (see e.g., the discussion in [72]). Finally, the uncertainties on the  $\text{FWHM}(\text{H}\beta)$  values of some sources reported in [15] are quite large, making their classification uncertain. For these reasons some of the sources included in that catalog can be considered just as candidate NLSy1 and not bona-fide NLSy1, including the three FSRQ tentatively re-classified by [59] and the  $\gamma$ -ray sources NVSS J093241+530633 and NVSS J095820+322401 reported in [59]<sup>4</sup>. In order to investigate the properties of the  $\gamma$ -ray-emitting NLSy1, it is important to start considering only bona-fide NLSy1, not mixing these

<sup>4</sup> In the same way, 3C 286 is classified as a Compact Steep Spectrum source in the 4FGL, while it is tentatively re-classified as a NLSy1 in [73,74]. The  $\text{FWHM}(\text{H}\beta)$  value reported in [74] exceeds the historical threshold of  $2000 \text{ km s}^{-1}$ , therefore 3C 286 could be considered as a candidate NLSy1. It is worth nothing also that the inclination angle between the jet and our line of sight is 48 degrees [75], significantly different from the relatively small angles estimated for the  $\gamma$ -ray-emitting NLSy1.

sources with FSRQ tentatively re-classified as NLSy1 and candidate NLSy1. For this reason this review is focused on the nine bona-fide NLSy1 included in the 4FGL catalog.

Among the 9  $\gamma$ -ray-emitting radio-loud NLSy1, only one source, SBS 0846+513, is included in the Third catalogue of Hard *Fermi*-LAT sources (3FHL; [76]), based on 7 years of LAT data analysed in the 10 GeV–2 TeV energy range, with a photon index of  $2.93 \pm 0.71$  and a flux of  $(7.13 \pm 1.50) \times 10^{-11} \text{ ph cm}^{-2} \text{ s}^{-1}$ . There are no NLSy1 included in the Second *Fermi*-LAT catalog of High-Energy Sources (2FHL; [77]), based on 80 months of data in the 50 GeV–2 TeV energy range. The lack of  $\gamma$ -ray-emitting NLSy1 in the 2FHL is in agreement with the hard ( $\Gamma_\gamma > 2.2$ )  $\gamma$ -ray spectrum observed in the 0.1–300 GeV energy range over 8 years of *Fermi* operation (see Table 1) and the lack of detection at Very High Energy (VHE;  $E > 100$  GeV) by the current Cherenkov Telescopes.

Pre-*Fermi* observations of 1H 0323+342 by Whipple [78] and VERITAS [79] at VHE resulted in upper limits. Furthermore, 1H 0323+342 and PKS 2004–447 were not detected by H.E.S.S. during an AGN monitoring program [80]. With the advent of *Fermi*-LAT, flaring activity observed in the High Energy (HE;  $100 \text{ MeV} < 100 \text{ GeV}$ ) regime can trigger follow-up observations with the current generation of Imaging Atmospheric Cherenkov Telescope. VERITAS observed PMN J0948+0022 for  $\sim 5.5$  h during 6–13 January 2013 (see Figure 2, left panel), a few days after the  $\gamma$ -ray flare observed by *Fermi*-LAT on 1 January 2013, and could set an upper limit of  $F_{>0.2\text{TeV}} < 4 \times 10^{-12} \text{ ph cm}^{-2} \text{ s}^{-1}$  [61] (see Figure 2, right panel). The lack of detection of PMN J0948+0022 at VHE could be due to different reasons: (1) The distance of the source ( $z = 0.5846$ ) is relatively large and most of the GeV/TeV emission may be absorbed due to pair production from  $\gamma$ -ray photons of the source and the infrared photons from the extragalactic background light (EBL). However, it worth noting that at least three blazars, S3 0218+35 [81], PKS 1441+25 [82,83], and Ton 0599 [84] are detected at VHE at much larger distance. (2) Due to bad weather conditions, the VERITAS observations were carried out a few days after the peak of the HE  $\gamma$ -ray activity, thus covering only the last part of the MeV-GeV flare. (3) Considering the similarities with FSRQ, a bright BLR may be present in the  $\gamma$ -ray-emitting NLSy1. The presence of a BLR could produce a spectral absorption feature due to pair production, which may either suppress all  $\gamma$ -rays above a few GeV, or manifest as a harder spectrum towards the VHE regime. The geometry of the BLR does not affect the possible detection at VHE because the important parameter is the angle at which the jet sees the BLR (e.g., [7,85,86]). However, the detection of FSRQ at VHE [84,87–92] has shown that the spectrum of FSRQ may extend to VHE energies during some flaring activities, indicating that the  $\gamma$ -rays may be produced outside the BLR during these high-activity periods. The same scenario may apply to the  $\gamma$ -ray-emitting NLSy1.

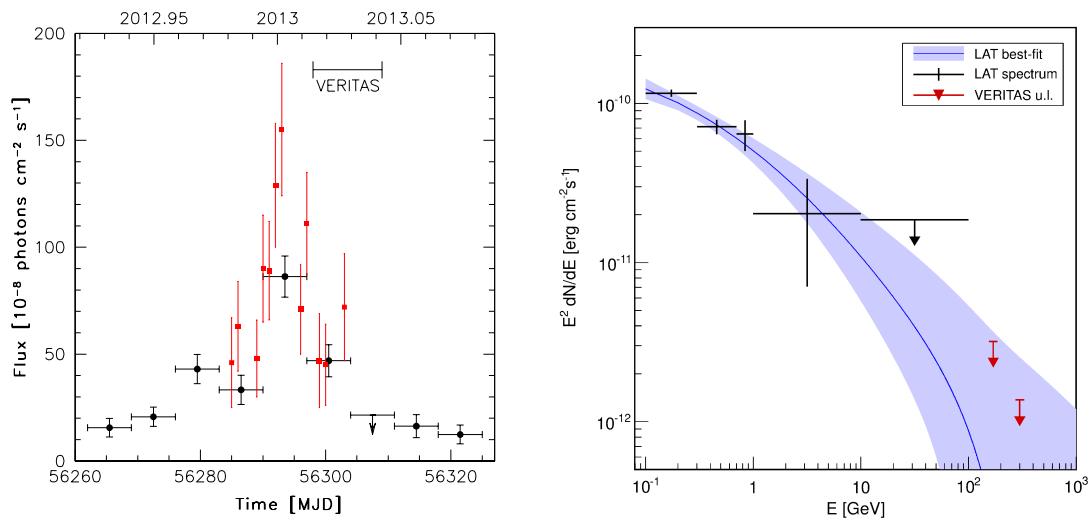


**Figure 2.** *Left panel:* LAT light curve of PMN J0948+0022 in the 0.1–100 GeV energy range during 1 December 2012– 31 January 2013, with 7-day time bins. Red solid squares represent daily fluxes reported for the period of high activity. The horizontal line indicates the period of the VERITAS observation. Adapted from [61]. *Right panel:* SED of PMN J0948+0022 in the MeV-to-TeV energy range. The LAT spectrum was extrapolated to the TeV energies and corrected for EBL absorption using the model of [93]. *Fermi*-LAT and VERITAS data points and upper limits are shown. Adapted from [61]. In both panels, arrow refers to  $2\text{-}\sigma$  upper limits. Upper limits are computed when  $TS < 10$ .

Future observations of  $\gamma$ -ray flaring NLSy1 observed by *Fermi*-LAT at VHE with the Cherenkov Telescope Array (CTA; [94]) and other future  $\gamma$ -ray satellites (e.g., AMEGO; [95]) will constrain the level of  $\gamma$ -ray emission of NLSy1 at 100 GeV or below. Preliminary simulations for follow-up observations of a sample of sources including bona-fide and candidate NLSy1 (not all of them with a confirmed detection in  $\gamma$ -rays by *Fermi*-LAT, see Section 2) have shown that SBS 0846+513, PMN J0948+0022, and PKS 1502+036 should be detected with CTA during high activity states in 50 h of observations [96].

### 3. X-ray Properties

The X-ray spectra of radio-quiet NLSy1 are usually characterized by a steep photon index ( $\Gamma_X > 2$ , [12,13]). The X-ray emission is one of the most intriguing aspects of the  $\gamma$ -ray-emitting NLSy1, with some differences observed with respect to FSRQ. The spectra are hard above 2 keV ( $\Gamma_X < 2$ ), which is similar to what is observed in FSRQ rather than radio-quiet NLSy1, suggesting that a significant contribution of inverse Compton (IC) radiation from a relativistic jet dominates that part of the X-ray spectrum. Differently from FSRQ, a narrow Fe line at 6.4 keV has been reported for one source, 1H 0323+342 (Figure 3, right panel), which has the softest X-ray spectrum of the  $\gamma$ -ray-emitting NLSy1 [97,98]. The majority of  $\gamma$ -ray-emitting NLSy1 for which good-quality X-ray spectra are available show an excess of emission at low energies with respect to the extrapolation of the hard X-ray spectral continuum model, making them different from typical blazars. As an example, the left panel of Figure 3 shows this excess below 2 keV in the X-ray spectrum of PMN J0948+0022. The 0.3–10 keV energy range spectra of  $\gamma$ -ray-emitting NLSy1 are usually well fitted by a broken power-law with a break around 2 keV [99]<sup>5</sup>, being the spectrum below the break due to disc/coronal emission, a typical feature of Seyfert

<sup>5</sup> In case of 1H 0323+342 a more complex X-ray spectrum was observed (e.g., [98]).

galaxies, and the emission above the break dominated by the jet emission, a typical feature of blazars. Photon indices obtained from power-law and broken power-law fits to the spectra of  $\gamma$ -ray-emitting NLSy1 observed with *XMM-Newton* are plotted in Figure 4. Only two of these sources do not have a significant soft excess: TXS 2116–077 [100] and PKS 2004–447 [101,102], although a tentative soft excess was reported in one of the two *XMM-Newton* observations performed in 2012 for the latter source [52]. None of the sources has shown evidence of intrinsic absorption in X-rays.

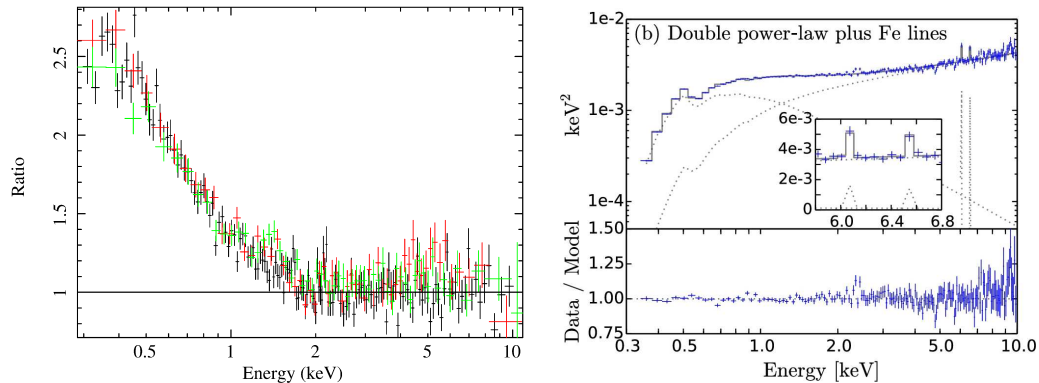


**Figure 3.** *Left panel:* *XMM-Newton* EPIC pn (black), MOS1 (red), and MOS2 (green) data of PMN J0948+0022 collected on 28–29 May 2011 shown as a ratio to a power law with photon index  $\Gamma = 1.48$ . Adapted from [103]. *Right panel:* data/model ratio for the *XMM-Newton* EPIC pn X-ray spectrum of 1H 0323+342 collected on 23–24 August 2015. A model including two power-laws and two Gaussian Iron emission lines with the Galactic value in the direction of the source fixed to  $N_{\text{H,Gal}} = 2.33 \times 10^{21} \text{ cm}^{-2}$  is applied to the data. Adapted from [98].

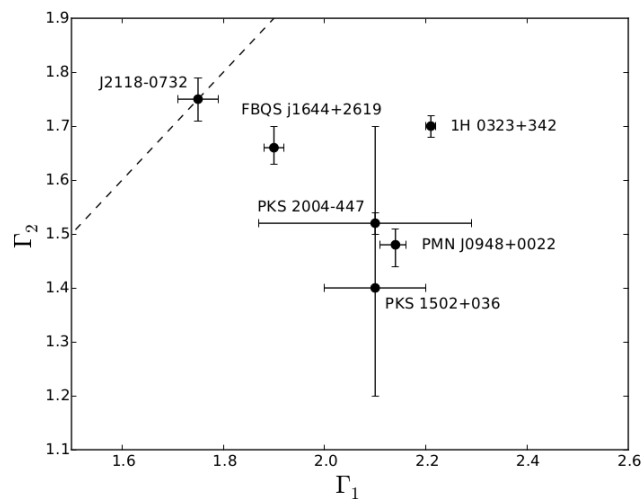


**Figure 4.** Photon indices obtained from broken power-law fits to *XMM-Newton* spectra of  $\gamma$ -ray-emitting NLSy1.  $\Gamma_1$  and  $\Gamma_2$  are the photon indices below and above the break, respectively. One of the sources is best described by a simple power-law. In case of 1H 0323+342 the broken power-law is just an approximation, as the spectrum show additional complexity. Adapted from [99].

A likely explanation for the X-ray spectra of  $\gamma$ -ray-emitting NLSy1 is that the underlying Seyfert emission, originating from the corona and accretion disc, has a noticeable contribution at low energies, the so-called soft X-ray excess. The origin of the soft X-ray excess is still an open issue both in radio-quiet and radio-loud AGN (e.g., [104]). Such a Seyfert component is a typical feature in the X-ray spectra of

radio-quiet NLSy1, but it is quite unusual in jet-dominated AGN, even if not unique (e.g., PKS 1510-089, [105]; 3C 273, [106]; 4C +04.42 [107]). The soft excess is often exceptionally strong in radio-quiet NLSy1, making it plausible that it would be detectable in the  $\gamma$ -ray-emitting radio-loud NLSy1 even though the jet emission is strong. In agreement with this, the analysis of the spectra of PMN J0948+0022 [103], FBQS J1644+2619 [99], and 1H 0323+342 [98] can be well described by models that include reflection and/or Comptonisation in addition to the jet emission. PMN J0948+0022 and 1H 0323+342 have shown breaks in the root-mean square (RMS)-variability around the spectral breaks, lending further support to a scenario where different components dominate at low and high energies [98,103]. Another possibility is that the soft X-ray emission originates from the jet itself. This could be the case if the tail of the synchrotron emission extends to the X-ray range, though the SED modelling of these sources does not favour this scenario (see Section 6). It has also been suggested that bulk Comptonization by a blob of plasma travelling along the jet could produce an excess at soft X-rays [108]. A similar feature has been proposed for the interpretation of the X-ray spectrum of the FSRQ PKS 1510+089 [105] and the candidate NLSy1 4C +04.42 [107]. However, this feature should be transient, in apparent contradiction with the fact that it is observed in the majority of sources. Currently, the reason for the differences between the X-ray spectra of  $\gamma$ -ray-emitting NLSy1 and FSRQ is under debate.

Further long-duration X-ray observations with *XMM-Newton* in conjunction with *NuSTAR* observations, preferably when the  $\gamma$ -ray activity of the source is low, will be needed to place stronger constraints on the models. A significant step forward in the study of the X-ray spectra of  $\gamma$ -ray-emitting NLSy1 will be obtained thanks to the next generation of X-ray satellites (i.e., Athena, XRISM, eXTP; [109–111]).

X-ray variability has been observed in most of the  $\gamma$ -ray-emitting NLSy1, in particular during high  $\gamma$ -ray activity periods (e.g., [38,61,63,65,112]), although not extreme and rapid as observed in radio-quiet NLSy1 (e.g., IRAS 13224–3809; [113]). The contemporaneous high activity level observed in X-rays and  $\gamma$ -rays suggests a co-spatiality of the emitting region, with the same mechanism (i.e., IC scattering) responsible for the radiation emitted in those energy bands, as observed in several FSRQ (e.g., [114–116]).

At hard X-rays only one  $\gamma$ -ray-emitting NLSy1 is included in the *Swift*-BAT 105-month catalogue [117], 1H 0323+342, with a photon index of  $1.62 \pm 0.30$ . The source is included also in the Fourth IBIS/ISGRI Soft Gamma-ray Survey Catalog [118]. Moreover, PMN J0948+0022 is included in the preliminary 100-month *Swift*-BAT Palermo catalog<sup>6</sup>. Both sources are detected in hard X-rays by *NuSTAR* during pointing observation [119,120], together with PKS 2004–447 [121].

#### 4. Infrared and Optical Properties

Different components (star formation activity, relativistic jet, and dusty torus) can contribute to the infrared emission of radio-loud NLSy1. Thanks to the all sky survey carried out by the *Wide-field Infrared Survey* (*WISE*) satellite a dedicated study of the infrared properties of a sample of 42 radio-loud NLSy1 has been performed by [122], confirming that infrared colours can be reproduced by a combination of AGN (dusty torus and relativistic jet) and host galaxy emission (star-formation emission). In particular, the infrared colours of  $\gamma$ -ray-emitting NLSy1 in that sample (i.e., 1H 0323+342, SBS 0846+513, PMN J0948+0022, PKS 1502+036, FBQS J1644+2619, and PKS 2004–447) have shown properties similar to FSRQ, with a dominance of the jet emission component in the infrared band [122].

By investigating *WISE* data, rapid infrared variability has been detected in some  $\gamma$ -ray-emitting NLSy1. In particular, [123] found infrared intraday variability in SBS 0846+513 and PMN J0948+0022,

---

<sup>6</sup> [http://bat.ifa.inaf.it/100m\\_bat\\_catalog/100m\\_bat\\_catalog\\_v0.0.htm](http://bat.ifa.inaf.it/100m_bat_catalog/100m_bat_catalog_v0.0.htm).

with an amplitude of  $\sim 0.1$ – $0.2$  mag and an emitting region size obtained by causality argument as  $< 10^{-3}$  pc, significantly smaller than the scale of the torus but consistent with an origin from the jet base. A similar variability amplitude was observed on a monthly time-scale for PKS 1502+036. Rapid infrared variability over a time-scale consistent with the jet-emitting region has been observed also in TXS 2116–077 by WISE [100].

Optical intraday variability has been reported for PMN J0948+0022 [124–127], SBS 0846+513 [128,129], PKS 1502+036 [127], and 1H 0323+342 [130,131]<sup>7</sup>. On the other hand, no intraday variability has been observed in optical for PKS 1502+036 [131].

For PMN J0948+0022, optical polarization as high as 36% [124] has been observed, with minute time-scale polarization variability but no variation of the electric vector position angle (EVPA). This has been interpreted as evidence of synchrotron emission from a compact region of highly ordered magnetic field. Polarization as high as 10% and intraday variation have been observed also in SBS 0846+513, accompanied by a rapid change of the EVPA [128].

During an optical polarimetry monitoring of 1H 0323+342 after the high  $\gamma$ -ray activity state observed by *Fermi*-LAT in July 2013 and lasted  $\sim 20$  days, the polarization of the source increased only to  $\sim 3\%$  [130]. A similar low polarization value has been observed by [132]. The variable polarized emission has confirmed the synchrotron origin for the optical emission, although the low optical polarization level of the source is probably due to the contamination from the thermal emission from the accretion disc. The optical EVPA was parallel to the jet orientation, implying a magnetic field direction, associated with the optical emission, perpendicular to the jet axis [130]. This implies either a presence of helical/toroidal magnetic field or a magnetic field compressed by transverse shock propagating down the jet. The different behaviours observed in these sources should be investigated in more details. However, the lack of high cadence optical polarisation observations of radio-loud NLSy1 limits the possibility to perform a systematic population study.

Periods of significant polarisation amplitude and angle variability have been reported in [132] for the  $\gamma$ -ray-emitting NLSy1 1H 0323+342, SBS 0846+513, PMN J0948+0022, and PKS 1502+036. Moreover, the EVPA of 1H 0323+342 has shown a preferential orientation (at 49.3 degrees to the position angle of the 15 GHz radio jet) similar to what was observed in high-synchrotron-peaked blazars [133]. The projected magnetic field of 1H 0323+342 is oriented at 40.7 degrees to the jet axis. This misalignment can be due to a combination of poloidal and toroidal field components.

Three long rotations of the polarisation angle have been observed in PKS 1502+036 and 1H 0323+342. Although the observed behaviour can be induced by noise, an intrinsic evolution of the EVPA is the most likely explanation of the observed behaviour. Rotations of the optical polarization plane have been observed in blazars, most of the time associated with high  $\gamma$ -ray activity (e.g., [134–137]). This behaviour has been explained by different theoretical scenarios: rotation of the emitting region on a helical trajectory (e.g., [137]), propagation in large-scale bent jet (e.g., [134]), turbulent processes resulting in random walks (e.g., [138]), light travel-time and projection effects within an axisymmetric emission region (e.g., [139]). Linear polarization observations of well sampled objects suggested that the relativistic jet in blazars contains a superposition of ordered helical magnetic fields and turbulent magnetic fields. In fact, high degree of polarization is expected in case of synchrotron radiation from a region of uniform magnetic field. The relatively low value of degree of optical polarization observed in blazars indicates that there is a mechanism in place that is the cause of disorder in magnetic field, like the turbulence. On the other hand, the constancy of EVPA in some periods supports the action of a process that partially

---

<sup>7</sup> Optical intraday variability in this source has been reported also in [65]. However, the contamination of the host galaxy has not been considered in the aperture photometry analysis used for producing the light curve of the source, making the results doubtful.

orders the magnetic field, like a shock or a helical magnetic field pattern, superposed to the turbulence. The observed patterns can be connected to the different contribution of the ordered and turbulent magnetic fields and the presence of shocks or not. These observed patterns can be compared to simulated light curves produced by the Turbulent Extreme Multi-Zone model to describe the time-dependent polarization of blazars (e.g., [140]). Long-term monitoring campaigns with more accurate observations are needed to compare the observed polarization data to simulated light curves in  $\gamma$ -ray-emitting NLSy1 and to provide clear evidence of similarity with blazars in their optical polarization variability.

The optical and UV part of the spectrum of FSRQ is usually characterized by the thermal emission from an accretion disc, while in BL Lac objects the disc is radiatively inefficient, with no significant emission in this energy range (e.g., [141]). The accretion disc emission is visible in the low activity state of the SED of PMN J0948+0022 [61], 1H 0323+342 [8], FBQS J1644+2619 [99], TXS 2116–077 [100], and PKS 1502+036 [63]. On the contrary, no significant evidence of thermal emission from the accretion disc has been observed in SBS 0846+513 [38] and PKS 2004–447 [102].

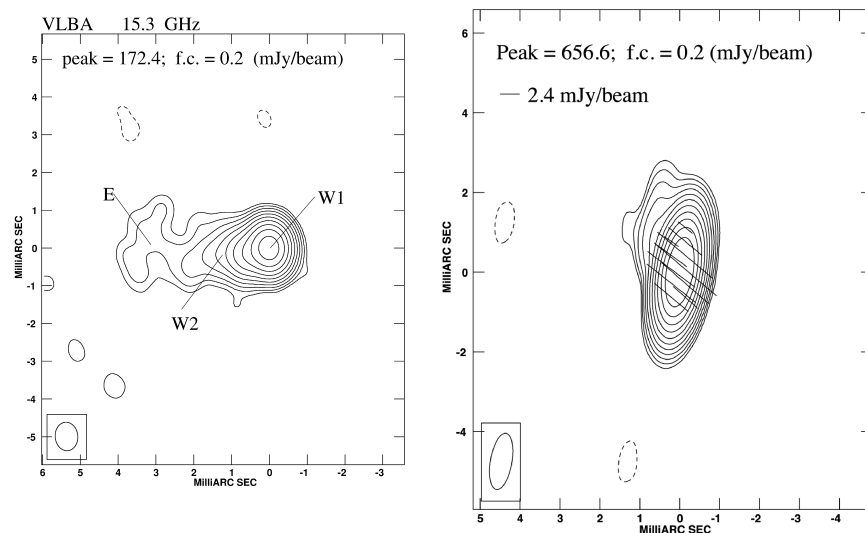


**Figure 5.** *Left panel:* VLBA image at 15 GHz of SBS 0846+513. Component W1 corresponds to the core region, component W2 to a knot in the jet, component E is an extended low-surface brightness structure with a steep spectrum. Adapted from [56]. *Right panel:* VLBA image at 15 GHz of PMN J0948+0022 collected on 2011 May 26. The vectors superimposed on the total intensity contours show the percentage polarization and the position angle of the electric vector. Adapted from [103]. In both images, it is provided the restoring beam, plotted in the bottom-left corner, the peak flux density in mJy/beam and the first contour (f.c.) intensity in mJy/beam, which is three times the off-source noise level. Contour levels increase by a factor of 2.

## 5. Radio Properties

On pc scale a core-jet structure has observed for SBS 0846+513 [56] (Figure 5, left panel), PKS 2004–447 [102,142], 1H 0323+342 [143,144], FBQS J1644+2619 [36,145], B3 1441+476 [146], PKS 1502+036 [147], and PMN J0948+0022 (Figure 5, right panel) [103,148], although the jet in the two latter sources is significantly fainter than that observed in the other sources. The pc scale morphology of  $\gamma$ -ray-emitting NLSy1 seems to be a reminiscent of blazars, suggesting Doppler boosting effect due to small jet viewing angles. Two-sided radio morphology has been seen at kpc scale in 1H 0323+342, PMN J0948+0022, and FBQS J1644+2619 [31,33,149]. This challenges the possible connection between compact steep spectrum (CSS) radio sources and radio-loud NLSy1, in particular  $\gamma$ -ray-emitting

NLSy1 being the aligned population of NLSy1 where the CSS properties are hidden by boosting effects (e.g., [16,29,53,102,146,150]). In the same way the X-ray spectrum of CSS sources is typically highly obscured with column density higher than  $10^{22} \text{ cm}^{-2}$  (e.g., [151]). The lack of evidence of intrinsic absorption in addition to the Galactic one in X-rays (see Section 3) disfavors a link between  $\gamma$ -ray-emitting NLSy1 and CSS sources.

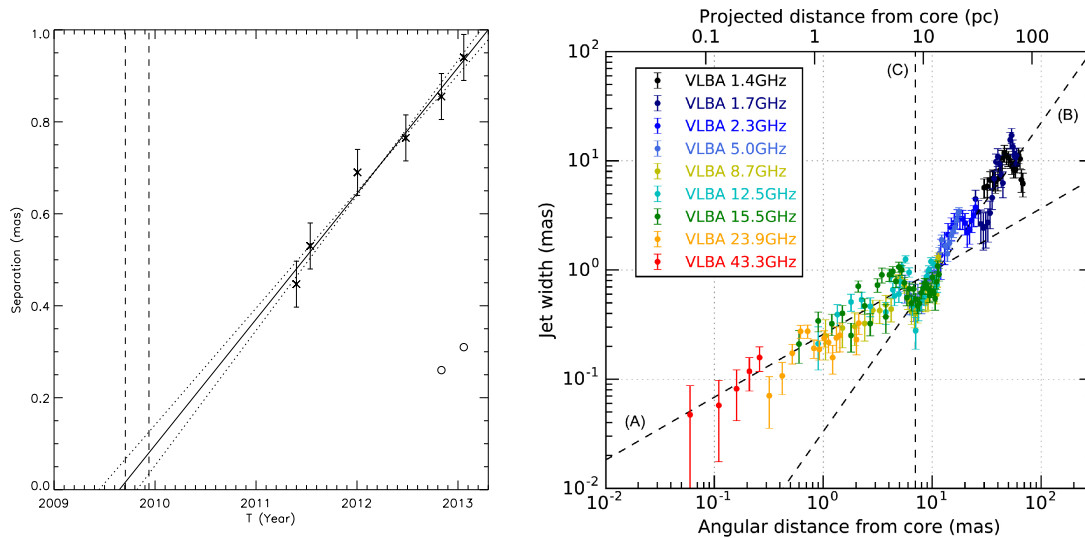


**Figure 6.** *Left panel:* The separation between the core component of SBS 0846+513 and the knot ejected in 2009 as a function of time. The solid line represents the regression fit to the 15 GHz VLBA MOJAVE data, while the dotted lines represent the uncertainties from the fit parameters. Dashed lines indicate the beginning and the peak of the radio flare observed by OVRO in 2009. Adapted from [38]. *Right panel:* Jet width profile of 1H 0323+342 as a function of (projected) distance  $z$  from the 43 GHz core. The dashed line (A) represents a best-fit model for the inner jet ( $z < 6.5$  mas), indicating a parabolic collimating jet. The dashed line (B) represents a best-fit model for the outer ( $z > 7.5$  mas) jet, indicating a hyperbolic expanding jet. The vertical dashed line (C) indicates the location of the quasi-stationary feature S. Adapted from [143].

The analysis of multi-epoch Very Long Baseline Interferometry (VLBI) data of SBS 0846+513 collected by the MOJAVE programme<sup>8</sup> during 2011–2013 pointed out a superluminal jet component moving away from the core with an apparent velocity of  $(9.3 \pm 0.6)c$  [38] (Figure 6, left panel), in agreement with the results presented in [39]. This apparent superluminal velocity supports the presence of boosting effects for the jet of SBS 0846+513. Interestingly, the superluminal jet component was ejected close in time with a radio flare observed in December 2009 by the Owens Valley Radio Observatory (OVRO) but during a quiescent activity state in  $\gamma$ -rays, representing an example of knot emission not connected to any  $\gamma$ -ray flaring activity. On the other hand, a new jet component for SBS 0846+513 has been ejected close in time with the  $\gamma$ -ray flare occurred in June–July 2011. Highly superluminal features with an apparent velocity of  $\sim 9c$  have been reported also for PMN J0948+0022 and 1H 0323+342 [39,152,153]. On the contrary, no apparent superluminal motion has been detected for PKS 1502+036 during 2008–2012, although the radio spectral variability, the one-sided jet-like structure, and the  $\gamma$ -ray properties seem to require the presence of boosting effects [147]. The lack of significant

<sup>8</sup> <https://www.physics.purdue.edu/MOJAVE/>.

proper motion in PKS 1502+036 has been confirmed by [39], with only a sub-luminal component detected. This result seems to resemble the ‘Doppler factor crisis’ observed in bright TeV BL Lacs (e.g., [154,155]). However, the SED of PKS 1502+036, in particular the high Compton dominance<sup>9</sup> (see Section 6) does not resemble a TeV BL Lac, but an FSRQ. This may suggest the presence of a structured jet in this NLSy1, with different regions having different Lorentz factors (i.e., a fast spine and a slower layer) (see e.g., [156]). Unfortunately, no Very Long Baseline Array (VLBA) monitoring was available during the  $\gamma$ -ray flaring activity of PKS 1502+036 observed in 2016 [63] to investigate the possible ejection of a new superluminal jet component during high  $\gamma$ -ray states.

A low fractional polarization compared to BL Lacs and FSRQ has been obtained by the analysis of the core linear polarization properties of 4  $\gamma$ -ray-emitting NLSy1 (i.e., 1H 0323+342, SBS 0846+513, PMN J0948+0022, and PKS 1502+036) using 15 GHz VLBA data. In addition, large misalignment between the core EVPA direction and the inner jet position angle has been observed in these 4 sources, similarly to what was observed in FSRQ. This can be related to a similarity with FSRQ in shock strength and geometry, with a standing transverse shock at the base of the jet which collimates the jet magnetic field perpendicular to the jet direction [157]. For 1H 0323+342, the nearest  $\gamma$ -ray-emitting NLSy1, the morphology of the inner jet obtained by using high-resolution multifrequency VLBA observations is well characterized by a parabolic shape up to 7 mas, an indication that the jet is continuously collimated near the base of the jet (Figure 6, right panel). Beyond 7 milliarcsecond (mas) the jet expands more rapidly at larger scales, transitioning into a hyperbolic/conical shape [143]. The acceleration and collimation zone seem to co-exist in this source, ending up with a bright quasi-stationary feature at 7 mas (a deprojected distance of  $\sim 100$  pc) corresponding to a recollimation shock [152]. The recollimation shock may be a possible site of  $\gamma$ -ray emission, similar to what is observed with HST-1 for the radio galaxy M87 (e.g., [158]). This may be an indication of a common jet formation mechanism for the two sources. The location of the  $\gamma$ -ray emitting region on a standing shock located far away from the SMBH has been proposed also for some BL Lacs (e.g., [137,159]) and FSRQ (e.g., [160,161]).

Strong radio variability has been observed at 15 GHz during the monitoring of the OVRO 40-m telescope of PMN J0948+0022 [61,103], PKS 1502+036 [147], and SBS 0846+513 [38,56]. An inferred variability brightness temperature of  $2.5 \times 10^{13}$ ,  $1.1 \times 10^{14}$ , and  $3.4 \times 10^{11}$  K is obtained for PKS 1502+036, SBS 0846+513, and PMN J0948+0022, respectively. A variability brightness temperature of  $7.0 \times 10^{11}$  K has been obtained for 1H 0323+342 during the monitoring by the Yamaguchi 32-m radio telescope [144]. In case of PKS 2004–447 a variability brightness temperature of  $1.7 \times 10^{14}$  K has been derived by [102] by using VLBA and Very Large Array (VLA) observations, in agreement with the results obtained based on the Ceduna monitoring [52]. These values are larger than the brightness temperature derived for the Compton catastrophe [162], suggesting that the radio emission of the jet is Doppler boosted. On the other hand, a high variability brightness temperature of  $10^{13}$  K, comparable to that of  $\gamma$ -ray-emitting NLSy1, has been observed for TXS 1546+353. However, no  $\gamma$ -ray emission has been detected from that source so far [102]. The brightness temperature derived from the 1.7 GHz VLBI flux density of the unresolved core of FBQS J1644+2619 ( $7 \times 10^9$  K) is too high for free-free emission, indicating that non-thermal processes dominate the radio emission, but lower than the limit value predicted by the Compton catastrophe [57].

An intensive monitoring of the  $\gamma$ -ray-emitting NLSy1 1H 0323+342, SBS 0846+513, PMN J0948+0022, and PKS 1502+036 from 2.6 GHz to 142 GHz with the Effelsberg 100-m and IRAM 30-m telescopes showed, in addition to an intensive variability, spectral evolution across the

---

<sup>9</sup> Compton dominance is the ratio of the peak Compton luminosity to peak synchrotron luminosity.

different bands following evolutionary paths which can be explained by shocks operating in a plasma outflow. These are typical characteristics seen in blazars [163].

## 6. SED Modelling

The first SED collected for the four NLSy1 detected in the first year of *Fermi*-LAT operation showed clear similarities with blazars: a double-humped shape with a first peak in the infrared/optical band due to synchrotron emission, a second peak in the MeV/GeV band likely due to IC emission, and an additional component related to the accretion disc in UV for three of the four sources (Figure 7). The physical parameters of these NLSy1 are blazar-like, and the jet powers are in the range of values usually observed in blazars [8]. Further studies confirmed that the physical parameters of  $\gamma$ -ray-emitting NLSy1 are blazar-like, in particular they seem to resemble FSRQ at the low-end of their BH mass distribution, with the dominant mechanism for producing the  $\gamma$ -ray emission being the IC scattering of seed photons from BLR or the dusty torus and the jet power being lower than the values estimated for FSRQ (e.g., [38,61,63,64,103]).

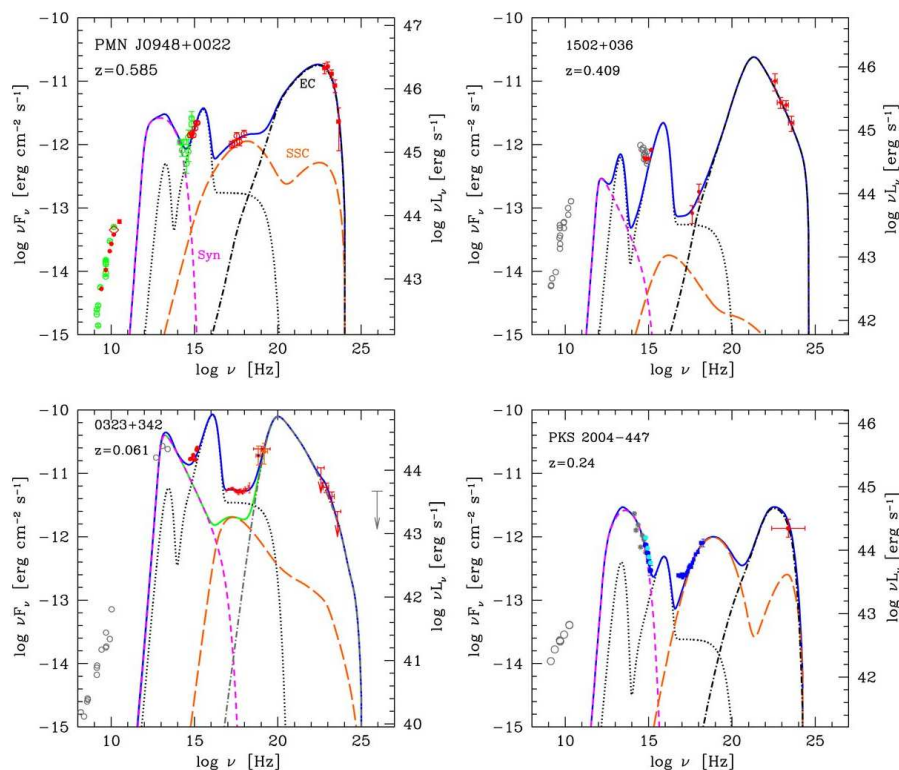


**Figure 7.** SED of the four NLSy1 detected by *Fermi*-LAT during the first year of operation. The synchrotron self-absorption is clearly visible around  $10^{11-12}$  Hz. The short dashed light blue line indicates the synchrotron component, while the long dashed orange line is the synchrotron-self Compton emission. The dot-dashed line refers to external Compton emission and the dotted black line represents the contribution of the accretion disc, X-ray corona and the infrared torus. The continuous blue line is the sum of all the contributions. Adapted from [8].

For PMN J0948+0022 the broad-band SED of the 2013 flaring activity state has been compared with that from an intermediate activity state observed in 2011 in [103] (Figure 8). Contrary to what was observed for some FSRQ (e.g., PKS 0537–441; [164]) the SED of the two activity states, modelled

as synchrotron emission and external Compton scattering of seed photons from a dust torus, could not be modelled by changing only the electron distribution parameters. A higher magnetic field is needed for the high activity state, consistent with the modelling of different activity states of the FSRQ PKS 0208–512 [165]. The 2013 flaring state has been modelled also assuming external Compton scattering of BLR photons. The model reproduces the data as well as the scattering of the IR torus photons, but requires magnetic fields which are far from equipartition [61]. On the other hand, external Compton scattering of BLR photons has been proposed as main mechanism for producing the high-energy emission in case of the first  $\gamma$ -ray flare observed by the same source in July 2010 [64]. In the same way, the  $\gamma$ -ray emission from 1H 0323+342 has been modelled with external Compton scattering of BLR photons. For this source a significant contribution from the X-ray corona has been taken into account to describe the X-ray part of the SED, at least during some periods [65,98].

The comparison of the SED of SBS 0846+513 during the flaring state in May 2012 with the SED built during a quiescent state is shown in the left panel of Figure 9. Similar to the case of PMN J0948+0022, the SED of the two different activity states, modelled by external Compton scattering of seed photons from a dust torus, could be fitted by changing the electron distribution parameters as well as the magnetic field [147]. A significant shift of the synchrotron peak to higher frequencies was observed during May 2012 flaring episode, similar to what has been observed in some FSRQ (e.g., PKS 1510–089, CTA 102; [166, 167]). On the other hand, contrary to what was observed for PMN J0948+0022, no significant evidence of thermal emission from the accretion disc has been observed in SBS 0846+513.

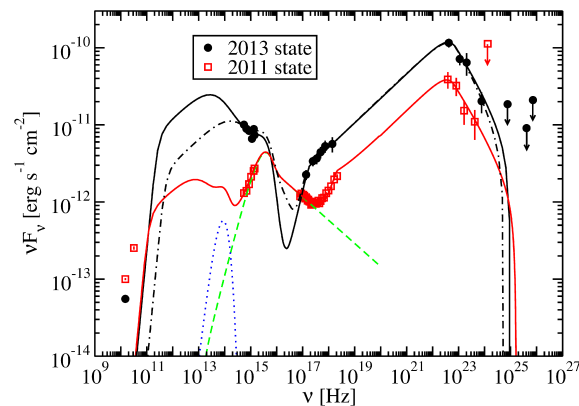


**Figure 8.** SED and models for the 2013 and 2011 activity states of PMN J0948+0022. The filled circles are the data from the 2013 flaring state, and the open squares are the data from the 2011 intermediate state taken from [103]. The dashed curve indicates the disc and coronal emission, and the dotted line indicates the thermal dust emission. Solid lines represent models consistent with scattering dust torus radiation, while the dashed-dotted curve represents a model consistent with the scattering of BLR radiation. Arrows refer to  $2\sigma$  upper limits on the source flux. The VERITAS upper limits are corrected for EBL absorption using the model of [93]. Adapted from [61].

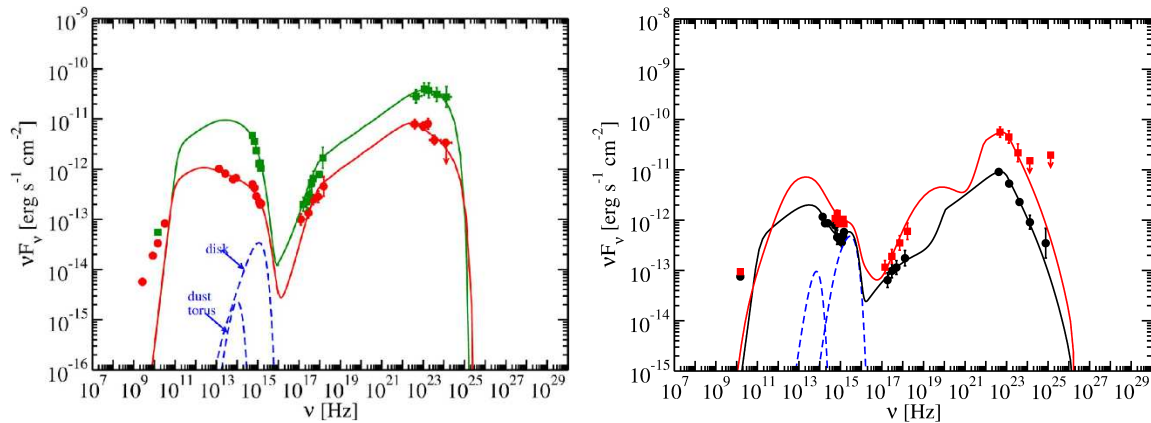


**Figure 9.** SED data (squares) and model fit (solid curve) of SBS 0846+513 (*left panel*) and PKS 1502+036 (*right panel*) in flaring activity with the thermal emission components shown as dashed curves. The data points were collected by OVRO at 15 GHz, *Swift* (UVOT and XRT) and *Fermi*-LAT. The SED in the quiescent state (taken from [56]) and average state, respectively, are shown as circles. Adapted from [147] (*left panel*) and [63] (*right panel*).

Two SED of PKS 1502+036 collected during an average activity state and the 2016 flaring state were compared in [63] (Figure 9, right panel). Most of the optical data in the SED are explained by synchrotron emission (together with a contribution from an accretion disc with a luminosity of  $6 \times 10^{44} \text{ erg s}^{-1}$ , a value lower than the luminosity usually observed for the disc of FSRQ as well as of the  $\gamma$ -ray-emitting NLSy1 PMN J0948+0022), the X-ray data by synchrotron self Compton emission, and the high-energy bump is modelled by an external Compton component with seed photons from a dust torus. Unlike the SED modelling reported in [67] for the same source, the magnetic field and Doppler factor are not changed simultaneously between the average and high activity state models in order to modify the minimum number of parameters between activity states. Moreover, jet powers for both the average and high states of PKS 1502+036 in [63] are near equipartition between the electron and magnetic field energy density, with the electron energy density being slightly higher in both cases. The two SED could be fitted by changing the electron distribution parameters as well as the magnetic field, similar to the case of the FSRQ PKS 2142–75 [168] and PKS 1424–418 [169] as well as the NLSy1 PMN J0948+0022 and SBS 0846+513 discussed in [61,147]. However, differently from those cases the magnetic field decreased during the flare with respect to the average state. The two SED of PKS 1502+036 show a Compton dominance  $\sim 10$ . A clear correlation between Compton dominance and the rest-frame peak synchrotron frequency was reported in [170] for blazars, related to the contribution of the external Compton component, which results to be higher for larger values of Compton dominance. The high value observed in PKS 1502+036 indicates that the external Compton emission is the main mechanism for producing  $\gamma$ -rays, as observed for several FSRQ (e.g., [170]). This confirms the similarities between  $\gamma$ -ray-emitting NLSy1 and FSRQ. A similar high Compton dominance has been observed in PMN J0948+0022 and SBS 0846+513 during low and high activity states [61].

As for SBS 0846+513, PMN J0948+0022, and PKS 1502+036, the high-energy bump of the SED of PKS 2004–447 is modelled with an external Compton scattering of dust torus seed photons in [102]. The disc luminosity of PKS 2004–447 obtained by the SED modelling is particularly weak,  $L_{\text{disc}} = 1.8 \times 10^{42} \text{ erg s}^{-1}$ , consistent with the value estimated on the basis of the optical spectrum [171]. Evidence has been building that IC on BLR photons is disfavored as the main  $\gamma$ -ray mechanism in FSRQ with respect to the IC on IR photons from the torus [85], in agreement with the SED modelling proposed for these  $\gamma$ -ray-emitting NLSy1.

## 7. Host Galaxy and BH Mass

The mechanisms for producing relativistic jets in radio-loud AGN are still unclear. In particular, the physical parameters that drive the jet formation are under debate. One of the key parameters should be the BH mass, with only large masses allowing an efficient jet formation [48]. Powerful relativistic jets are apparently only associated with the most massive SMBH ( $M_{\text{BH}} > 10^8 M_{\odot}$ ; e.g., [172]) hosted in elliptical galaxies. In a framework in which the jet is powered by energy extracted from the rotating SMBH (e.g., [173]), that can be interpreted as an evidence that efficient jet formation requires rapidly spinning SMBH, which can be obtained through major mergers [48]. In fact, higher spins are predicted due to spin-up for episodes of coherent accretion with a preferred orientation, as in the case of major mergers, while lower spins are expected for growth via minor mergers, in which the angular momentum is deposited from random directions. Indeed, major mergers are commonly observed in the elliptical galaxies producing the most powerful jets [174,175].

In this context the discovery of relativistic jets in radio-loud NLSy1 usually associated with relatively small BH masses challenges the current knowledge on how the jets are generated and developed (e.g., [46]). The estimates of the BH masses based on the virial method (i.e., on their luminosity and the width of their broad lines; e.g., [176]) for radio-loud NLSy1 are typically  $10^6$ – $10^7 M_{\odot}$  [16,42]. These estimates suggest two possible interpretations: either radio-loud NLSy1 correspond to a fundamentally different mechanism for the formation of relativistic jets or alternatively the BH mass in radio-loud NLSy1 is largely underestimated.

The BH mass of radio-loud NLSy1 might be underestimated due either to the effect of radiation pressure on BLR clouds [22] or to projection effects which reduces the width of their broad lines (e.g., [23,51]). The effect of flattening of the BLR on the virial mass estimate may be larger in  $\gamma$ -ray-emitting NLSy1 that should have small angle of view, as suggested by their blazar-like behaviour. Higher BH masses are instead in agreement with the values estimated by modeling the optical and UV data with a Shakura and Sunyaev disc spectrum (e.g., [177]). A possibility way to reduce the discrepancy between the BH mass values obtained with the virial method and those obtained by the disc modelling method is to assume a radiatively efficiency of the disc significantly lower than the 10% value usually observed for blazars [178].

For PKS 1502+036 a BH mass of  $\sim 7 \times 10^8 M_{\odot}$  has been obtained from the near-infrared bulge luminosity of the host galaxy [179]. From its optical spectrum and the BLR radius–luminosity relation by [180], a virial mass of  $4 \times 10^6 M_{\odot}$  has been estimated by [16]. On the other hand, by modelling the optical–UV data with a Shakura and Sunyaev accretion disc spectrum, [177] found  $M_{\text{BH}} = 3 \times 10^8 M_{\odot}$ , compatible with the value obtained by the near-infrared bulge luminosity within the uncertainties.

Conflicting results were also obtained for FBQS J1644+2619, with a BH mass of  $2.1 \times 10^8 M_{\odot}$  obtained by the near-infrared bulge luminosity [121], significantly larger than the virial estimate ( $0.8$ – $1.4 \times 10^7 M_{\odot}$ ; [16,171]), but compatible with the value obtained from the modelling of the accretion disc emission ( $1.6 \times 10^8 M_{\odot}$ ; [177]). Similarly, for 1H 0323+342 values in the range  $(1.5$ – $2.2) \times 10^7 M_{\odot}$  were estimated from near-infrared and optical spectroscopy [120], while values of  $(1.6$ – $4.0) \times 10^8 M_{\odot}$  were obtained by the near-infrared bulge luminosity [181].

It appears that the BH masses estimated with the virial method in  $\gamma$ -ray-emitting NLSy1 are systematically and significantly smaller than those derived from other techniques. It is worth mentioning that fitting the optical–UV spectrum of a sample of both radio-quiet and radio-loud NLSy1 (including 4 of the 9  $\gamma$ -ray-emitting NLSy1) with the standard Shakura & Sunyaev accretion disc, [24] has obtained BH masses that are about an order of magnitude larger than their virial estimates. A higher BH mass estimation may solve the problem of the minimum BH mass required for the formation of relativistic jets, but it leaves open the host galaxy issue. Spiral galaxies are usually formed by secular processes,

with central BH masses typically ranging between  $10^6$ – $10^7 M_{\odot}$  (e.g., [182,183]), so it would not be clear how powerful relativistic jets could form in spiral galaxies. Host galaxy studies of NLSy1 have mostly concentrated on radio-quiet objects (e.g., [43,184]): most of them are found in disc-like galaxies (e.g., [40]). However, only a handful of radio-loud NLSy1 have been investigated so far.

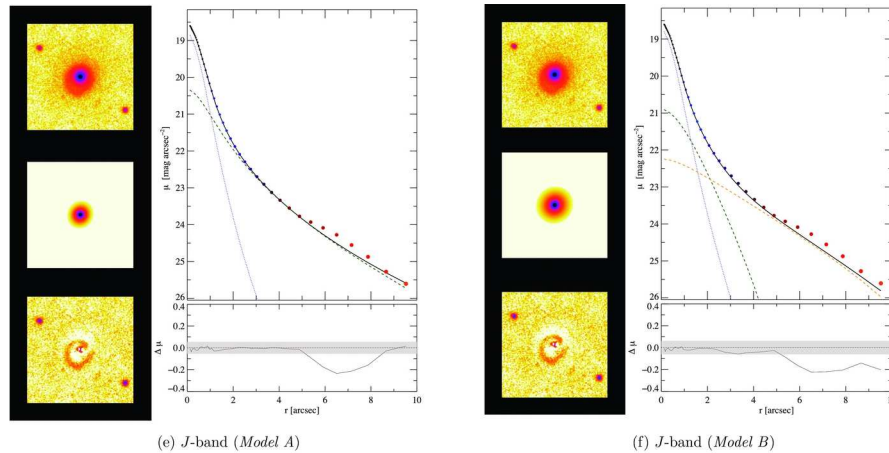


**Figure 10.** Two-dimensional surface-brightness profile decomposition of 1H 0323+342 in *J*-band for Model A (PSF+Bulge; *left panel*) and Model B (PSF+Bulge+Disc; *right panel*). *Top left subpanel*: the observed image in a field of view of 20 arcsec  $\times$  20 arcsec. *Middle left subpanel*: model used to describe the surface brightness distribution. *Bottom left subpanel*: the residual image. *Top right subpanel*: radial profile of the surface brightness distribution. The filled circles show the observations, and the solid, pointed, and dashed lines represent the model, PSF, and host galaxy, respectively. The exponential disk component is shown in orange. *Bottom right subpanel*: residuals. Adapted from [181].

The morphology of the host galaxy has been determined only for 5 radio-loud NLSy1, four of them detected in  $\gamma$ -rays by *Fermi*-LAT. Observations of 1H 0323+342 with the Hubble Space Telescope and the Nordic Optical Telescope (NOT) revealed a structure that may be interpreted either as a one-armed galaxy [185] or as an elliptical galaxy with residual of a galaxy merger [181] (Figure 10). In the case of PKS 2004–447, near-infrared observations with ISAAC mounted on Very Large Telescope (VLT) suggested that the host may have a pseudo-bulge morphology [186]. This should imply that the relativistic jet in PKS 2004–447 is launched from a pseudo-bulge via secular processes, in contrast to the theoretical models proposed for the jet production. However, the surface brightness distribution of the host is not well constrained by a bulge+disc model, leaving the debate on its morphology at large radii ( $>1.5$ – $2$  arcsec) still open.

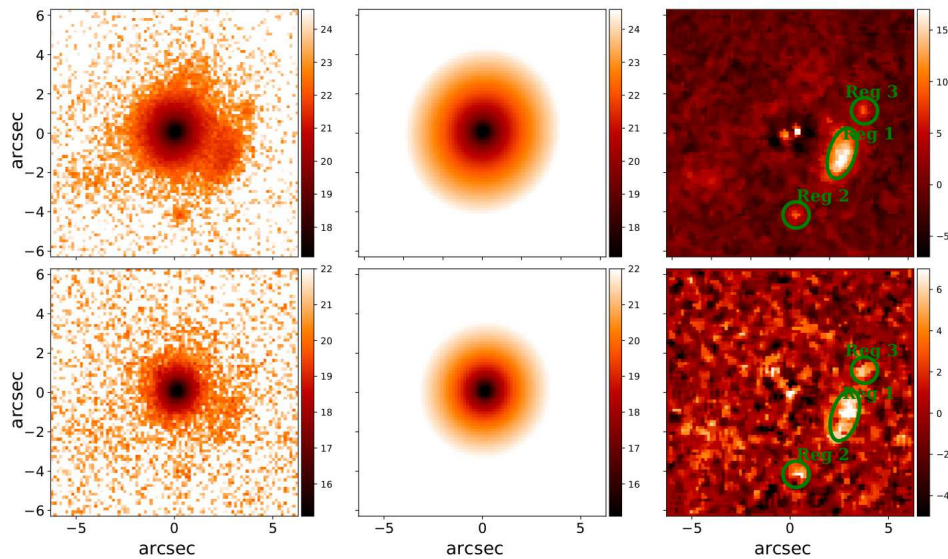


**Figure 11.** *Left panels:* central  $13 \times 13 \text{ arcsec}^2$  of the images in the  $J$  and  $K_s$  band of PKS 1502+036, top and bottom, respectively. *Center panels:* GALFIT models using a Sérsic profile combined with a nuclear PSF. *Right panels:* residual images after subtracting the model. Colour bars are in  $\text{mag arcsec}^{-2}$  (left-hand and centre panels). Adapted from [179].

Observations of FBQS J1644+2619 in  $J$  and  $K_s$  bands with the NOT by [187] suggested that the source resides in a barred lenticular galaxy. However, deeper near-infrared observations of FBQS J1644+2619 in  $J$  band have been obtained using the Canarias InfraRed Camera Experiment (CIRCE) at the Gran Telescopio Canarias [121]. The 2D surface brightness profile of the source is modelled up to 5 arcsec by the combination of a nuclear and a bulge component with a Sérsic index of 3.7, indicative of an elliptical galaxy. The structural parameters of the host are consistent with the correlations of effective radius and surface brightness against absolute magnitude measured for elliptical galaxies. From the infrared bulge luminosity [188] a BH mass of  $(2.1 \pm 0.2) \times 10^8 M_\odot$  has been estimated. All these pieces of evidence strongly indicate that the relativistic jet in FBQS J1644+2619 is produced by a massive SMBH in an elliptical galaxy, as expected for radio-loud AGN. Galaxies residing in denser large-scale environments are preferably ellipticals (e.g., [189,190]). It is worth mentioning that FBQS J1644+2619 lies in a supercluster environment<sup>10</sup>, as well as many radio-loud NLSy1, with a trend of increasing radio loudness with increasing large-scale environment density. Under the assumption that the large-scale environment may have an impact on the galaxy evolution, and therefore the production of jet, the dense large-scale environment of FBQS J1644+2619 is in agreement with the fact that the source is hosted in an elliptical galaxy [191]. The analysis of observations in  $J$  and  $K_s$  bands with the Infrared Spectrometer And Array Camera (ISAAC) on VLT of PKS 1502+036 (Figure 11) has shown that its surface brightness profile, extending to  $\sim 20$  kpc, is modeled by the combination of a nuclear and a bulge component with a Sérsic profile with index  $n = 3.5$ , which is indicative of an elliptical galaxy (Figure 12). From the near-infrared

<sup>10</sup> Private communication by E. Järvelä.

bulge luminosity a BH mass of  $\sim 7 \times 10^8 M_{\odot}$  has been estimated. A circumnuclear structure observed near PKS 1502+036 may be the result of a galaxy interaction [179].

Near-infrared observations of the host galaxy of SDSS J161259.83+421940.3 (not detected in  $\gamma$ -rays so far) with NOT in  $J$ -band suggested a structure consistent with either a spiral arm or a morphological disturbance due to a recent merger, and a BH mass of  $\sim 8 \times 10^6 M_{\odot}$  [192]. This is in agreement with the fact that  $\gamma$ -ray-emitting radio-loud NLSy1 (with a powerful relativistic jet) and radio-loud NLSy1 not able to emit in  $\gamma$ -rays (with a less powerful jet) can be part of different populations. Tentative investigation of the host galaxy of SBS 0846+513 [59] and TXS 2116–077 [100] by using SDSS images is not conclusive and strongly limited by the low resolution of the SDSS images for sources at redshift  $z > 0.2$ .

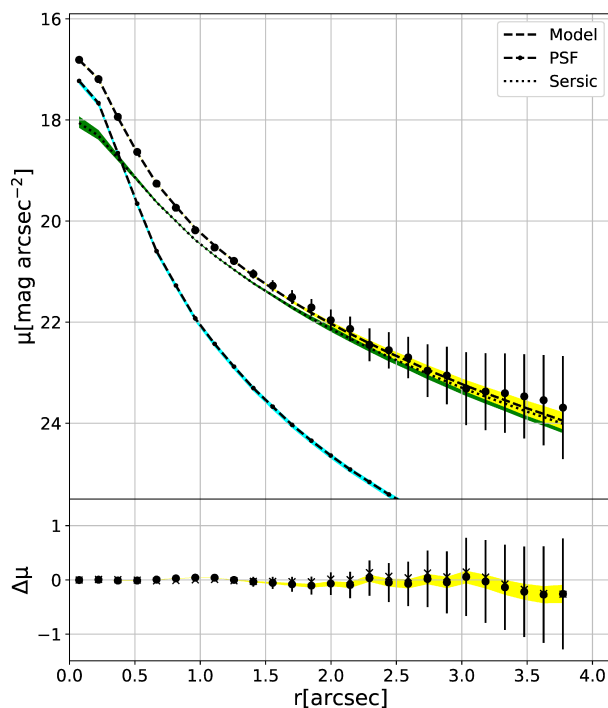


**Figure 12.** Surface brightness decomposition in the  $J$ -band of PKS 1502+036. The observed profiles are the black dots, the nuclear PSF is the dot–dashed light blue curve, the bulge component is reproduced with a Sérsic model (green dot line). In the bottom panels the residuals are shown. In the residual panel crosses represent bulge + disc component. Adapted from [179].

For two of the nine  $\gamma$ -ray-emitting NLSy1 there is evidence that they reside in elliptical galaxies with a BH mass higher than  $10^8 M_{\odot}$ , similar to blazars. A possible scenario is that powerful relativistic jets can be produced only in radio-loud NLSy1 residing in elliptical galaxies. However, the lack of information about the host galaxy for about half of the  $\gamma$ -ray-emitting NLSy1 together with some contrasting results indicate that the controversy on which galaxies host radio-loud NLSy1 is still open. In addition, a BH mass of  $3\text{--}4 \times 10^7 M_{\odot}$  has been derived for 1H 0323+342 from reverberation mapping results obtained with the Lijiang 2.4-m telescope by [193]. However, uncertainties on such a kind of measurements due to the effect of high accretion rate on the dynamics and geometry of the BLR in NLSy1 together with the adequacy of the cadence of the reverberation mapping campaign (e.g., [194]) and the virial factor used (e.g., [195]) should be careful taken into account. In case the low value of the BH mass estimated

is confirmed, this would suggest that even low mass SMBH can produce powerful relativistic jets and represent a dramatic change in our view of radio-loud AGN. In fact, the connection between very massive SMBH and powerful radio emission is not purely an empirical threshold on the BH mass. It is becoming increasingly clear that radio-loud AGN are the result of a specific path of galaxies evolution, involving mergers, coalescence and spin-up of SMBH (e.g., [174,196]). These mechanisms are expected to operate only at the high end of the galaxies mass distribution, and, consequently, only in the presence of very massive black holes. Only a handful of powerful radio galaxies have been found in spirals (e.g., [197,198]), all of them with BH mass higher than  $10^8 M_{\odot}$ . Genuine low mass SMBH producing a radio-loud AGN would represent a strong challenge to this picture.

## 8. Conclusions

The discovery of  $\gamma$ -ray emission from radio-loud NLSy1 has raised important questions about the nature of these sources, the conditions that lead to powerful jet formation and the mechanisms that produce the high-energy emission in these objects. Observations with the *Fermi Gamma-ray Space Telescope* have revealed NLSy1 as a possible new class of  $\gamma$ -ray-emitting AGN with blazar-like properties [8]. It is a small class, consisting of only 9 bona-fide NLSy1 to date [3]. The continuous all-sky survey in  $\gamma$ -rays by *Fermi*-LAT will allow us to identify new  $\gamma$ -ray-emitting NLSy1 and to better characterize already known  $\gamma$ -ray sources belonging to this intriguing class of objects. However, the search of transient  $\gamma$ -ray activity from NLSy1 by generating weekly and monthly light curve has not been effective yet [e.g., 199]. In addition, a careful analysis of the current and future spectroscopical optical survey data is important to identify new bona-fide radio-loud NLSy1. In this context, SDSS-V will be an all-sky multi-epoch spectroscopic survey of over six million objects [200] that allows an important step forward in the research and characterization of AGN classes including the NLSy1.

The  $\gamma$ -ray observations as well as the multi-wavelength properties of  $\gamma$ -ray-emitting NLSy1 provide clear evidence for the existence of powerful jets pointed close to our line of sight in these objects. Compared to the blazar population,  $\gamma$ -ray-emitting NLSy1 seems to be similar to FSRQ, but with lower jet powers. However, the estimated BH mass of radio-loud NLSy1 has large uncertainties. These uncertainties may influence the jet power and accretion rate estimates, and therefore the comparison with  $\gamma$ -ray-emitting blazars. The SED of  $\gamma$ -ray-emitting NLSy1 are Compton-dominated, with the high-energy emission mainly produced by external Compton of infrared torus, resembling the typical SED of FSRQ. Differently from the  $\gamma$ -ray spectra, in X-rays the spectra of  $\gamma$ -ray-emitting NLSy1 show not only the emission from the relativistic jet but also some Seyfert-like features from the accretion flow, like the soft X-ray excess and the Fe line in case of 1H 0323+342, unusual for blazars. A regular monitoring from radio-to- $\gamma$ -rays will be fundamental for continuing to investigate with great details the nature and emission mechanisms of these objects and to reveal further differences and similarities with blazars.

Understanding the nature of the host galaxies of  $\gamma$ -ray-emitting NLSy1 and estimating their BH mass are of great interest in the context of the models for the formation of relativistic jets [e.g., 201]. There are increasing evidence that the host of some radio-loud NLSy1, in particular  $\gamma$ -ray-emitting NLSy1, differ from those of radio-quiet NLSy1, usually spirals with low BH mass. In case of FBQS J1644+2619 and PKS 1502+036 the host is an elliptical galaxy with a BH mass higher than  $10^8 M_{\odot}$ , in agreement to what is observed in radio-loud AGN. Estimates of the BH mass obtained with different techniques (i.e., accretion disc model fitting, optical spectro-polarimetry, IR bulge luminosity) are larger than the virial masses of these  $\gamma$ -ray-emitting NLSy1. These results seem to confirm that a massive SMBH is a key ingredient for developing powerful relativistic jet and among the radio-loud NLSy1 only those hosted in massive elliptical galaxies are able to produce these structures. However, new high-resolution observations of the

host galaxies of other  $\gamma$ -ray-emitting NLSy1 will be fundamental to obtain further important insights into relativistic jet development.

**Author Contributions:** F.D. is the sole author of this publication.

**Funding:** This research received no external funding.

**Acknowledgments:** I would like to thank all my collaborators that have worked with me on NLSy1 over the years, in particular M. Orienti, J. Finke, C. M. Raiteri, J. Larsson, J. Acosta-Pulido, A. Capetti, M. Giroletti, T. Hovatta, E. Angelakis. This work was supported by the Korea's National Research Council of Science and Technology (NST) granted by the International joint research project (EU-16-001). I acknowledge financial contribution from the agreement ASI-INAF n. 2017-14-H.0 and from the contract PRIN-SKA-CTA-INAF 2016. This research has made use of NASA's Astrophysics Data System. This research has made use of the NASA/IPAC Extragalactic Database, which is funded by the National Aeronautics and Space Administration and operated by the California Institute of Technology. The Fermi LAT Collaboration acknowledges generous ongoing support from a number of agencies and institutes that have supported both the development and the operation of the LAT as well as scientific data analysis. These include the National Aeronautics and Space Administration and the Department of Energy in the United States, the Commissariat à l'Énergie Atomique and the Centre National de la Recherche Scientifique/Institut National de Physique Nucléaire et de Physique des Particules in France, the Agenzia Spaziale Italiana and the Istituto Nazionale di Fisica Nucleare in Italy, the Ministry of Education, Culture, Sports, Science and Technology (MEXT), High Energy Accelerator Research Organization (KEK) and Japan Aerospace Exploration Agency (JAXA) in Japan, and the K. A. Wallenberg Foundation, the Swedish Research Council and the Swedish National Space Board in Sweden. Additional support for science analysis during the operations phase is gratefully acknowledged from the Istituto Nazionale di Astrofisica in Italy and the Centre National d'Études Spatiales in France. This work performed in part under DOE Contract DE-AC02-76SF00515. This research has made use of the data from the MOJAVE database that is maintained by the MOJAVE team (Lister et al. 2009, AJ, 137, 3718). Based on observations obtained with XMM-Newton, an ESA science mission with instruments and contributions directly funded by ESA Member States and NASA. The National Radio Astronomy Observatory is a facility of the National Science Foundation operated under cooperative agreement by Associated Universities, Inc. I acknowledge the use of public data from the Swift data archive. Based on observations made with ESO Telescopes at the La Silla Paranal Observatory under programme 290.B-5045. Based on observations made with the GTC telescope, in the Spanish Observatorio del Roque de los Muchachos of the Instituto de Astrofisica de Canarias, under Director's Discretionary Time (proposal code GTC2016-053).

**Conflicts of Interest:** The authors declare no conflict of interest.

- Hartman, R.C.; Bertsch, D.L.; Bloom, S.D.; Chen, A.W.; Deines-Jones, P.; Esposito, J.A.; Fichtel, C.E.; Friedlander, D.P.; Hunter, S.D.; McDonald, L.M.; et al. The Third EGRET Catalog of High-Energy Gamma-Ray Sources. *Astrophys. J. Suppl. Ser.* **1999**, *123*, 77.
- Blandford, R.D.; Rees, M.J. Some comments on radiation mechanisms in Lacertids. In *Pittsburgh Conference on BL Lac Objects*; Wolfe, A.M., Ed. Pittsburgh: Pitts University of Pittsburgh Press **1978**, 328.
- Abdollahi, S.; Acero, F.; Ackermann, M.; Ajello, M.; Atwood, W.B.; Axelsson, M.; Baldini, L.; Ballet, J.; Barbiellini, G.; Bastieri, D.; et al. Fermi Large Area Telescope Fourth Source Catalog. *Astrophys. J. Suppl. Ser.* **2019**, *submitted*.
- Acero, F.; Ackermann, M.; Ajello, M.; Albert, A.; Atwood, W.B.; Axelsson, M.; Baldini, L.; Ballet, J.; Barbiellini, G.; Bastieri, D.; et al. Fermi Large Area Telescope Third Source Catalog. *Astrophys. J. Suppl. Ser.* **2015**, *218*, 23.
- Padovani, P. On the two main classes of active galactic nuclei. *Nat. Astron.* **2017**, *1*, 194.
- D'Ammando, F.; Orienti, M.; Finke, J.; Larsson, J.; Giroletti, M.; Raiteri, C.M. A Panchromatic View of Relativistic Jets in Narrow-Line Seyfert 1 Galaxies. *Galaxies* **2016**, *4*, 11.
- Abdo, A.A.; Ackermann, M.; Ajello, M.; Axelsson, M.; Baldini, L.; Ballet, J.; Barbiellini, G.; Bastieri, D.; Battelino, M.; Baughman, B.M.; et al. Fermi/Large Area Telescope Discovery of Gamma-Ray Emission from a Relativistic Jet in the Narrow-Line Quasar PMN J0948+0022. *Astrophys. J.* **2009**, *699*, 976.
- Abdo, A.A.; Ackermann, M.; Ajello, M.; Baldini, L.; Ballet, J.; Barbiellini, G.; Bastieri, D.; Bechtol, K.; Bellazzini, R.; Berenji, B.; et al. Radio-Loud Narrow-Line Seyfert 1 as a New Class of Gamma-Ray Active Galactic Nuclei. *Astrophys. J.* **2009**, *707*, L142.

9. Osterbrock, D.E.; Pogge, R.W. The spectra of narrow-line Seyfert 1 galaxies. *Astrophys. J.* **1985**, *297*, 166.
10. Goodrich, R.W. Spectropolarimetry of “Narrow-Line” Seyfert 1 Galaxies. *Astrophys. J.* **1989**, *342*, 224.
11. Pogge, R.W. Narrow-line Seyfert 1s: 15 years later. *New Astron. Rev.* **2000**, *44*, 381.
12. Boller, T.; Brandt, W.N.; Fink, H. Soft X-ray properties of narrow-line Seyfert 1 galaxies. *Astron. Astrophys.* **1996**, *305*, 53.
13. Grupe, D.; Komossa, S.; Leighly, K.M.; Page, K.L. The Simultaneous Optical-to-X-Ray Spectral Energy Distribution of Soft X-Ray Selected Active Galactic Nuclei Observed by Swift. *Astrophys. J. Suppl. Ser.* **2010**, *187*, 64.
14. Leighly, K.M. A Comprehensive Spectral and Variability Study of Narrow-Line Seyfert 1 Galaxies Observed by ASCA. II. Spectral Analysis and Correlations. *Astrophys. J.* **1999**, *125*, L317.
15. Rakshit, S.; Stalin, C.S.; Chand, H.; Zhang, X.-G. A Catalog of Narrow Line Seyfert 1 Galaxies from the Sloan Digital Sky Survey Data Release 12. *Astrophys. J. Suppl. Ser.* **2017**, *229*, 39.
16. Yuan, W.; Zhou, H.Y.; Komossa, S.; Dong, X.B.; Wang, T.G.; Lu, H.L.; Bai, J.M. A Population of Radio-Loud Narrow-Line Seyfert 1 Galaxies with Blazar-Like Properties? *Astrophys. J.* **2008**, *685*, 801.
17. Zhou, H.-Y.; Wang, T.-G.; Yuan, W.; Lu, H.; Dong, X.; Wang, J.; Lu, Y. A Comprehensive Study of 2000 Narrow Line Seyfert 1 Galaxies from the Sloan Digital Sky Survey. I. The Sample. *Astrophys. J. Suppl. Ser.* **2006**, *166*, 128.
18. Ferrarese, L.; Merritt, D. A Fundamental Relation between Supermassive Black Holes and Their Host Galaxies. *Astrophys. J.* **2000**, *539*, L9.
19. Gebhardt, K.; Bender, R.; Bower, G.; Dressler, A.; Faber, S.M.; Filippenko, A.V.; Green, R.; Grillmair, C.; Ho, L.C.; Kormendy, J.; et al. A Relationship between Nuclear Black Hole Mass and Galaxy Velocity Dispersion. *Astrophys. J.* **2000**, *539*, L13.
20. Grupe, D.; Mathur, S.  $M_{BH}-\sigma$  Relation for a Complete Sample of Soft X-Ray-selected Active Galactic Nuclei. *Astrophys. J.* **2004**, *606*, L41.
21. Mathur, S.; Kuraskiewicz, J.; Czerny, B. Evolution of active galaxies: Black-hole mass-bulge relations for narrow line objects. *New Astron.* **2001**, *6*, 321.
22. Marconi, A.; Axon, D.J.; Maiolino, R.; Nagao, T.; Pastorini, G.; Pietrini, P.; Robinson, A.; Torricelli, G. The Effect of Radiation Pressure on Virial Black Hole Mass Estimates and the Case of Narrow-Line Seyfert 1 Galaxies. *Astrophys. J.* **2008**, *678*, 693.
23. Decarli, R.; Dotti, M.; Fontana, M.; Haardt, F. Are the black hole masses in narrow-line Seyfert 1 galaxies actually small? *Mon. Notices R. Astron. Soc.* **2008**, *386*, L15.
24. Viswanath, G.; Stalin, C.S.; Rakshit, S.; Kurian, K.S.; Ujjwal, K.; Gudennavar, S.B.; Kartha, S.S. Are Narrow-line Seyfert 1 Galaxies Powered by Low-mass Black Holes? *Astrophys. J.* **2019**, *881*, L24.
25. Mejia-Restrepo, J.E.; Lira, P.; Netzer, H.; Trakhtenbrot, B.; Capellupo, D.M. The effect of nuclear gas distribution on the mass determination of supermassive black holes. *Nat. Astron.* **2018**, *2*, 63.
26. Capellupo, D.M.; Netzer, H.; Lira, P.; Trakhtenbrot, B.; Mejia-Restrepo, J. Active galactic nuclei at  $z \sim 1.5$  - I. Spectral energy distribution and accretion discs. *Mon. Notices R. Astron. Soc.* **2015**, *446*, 3472.
27. York, D.G.; Adelman, J.; Anderson, J.E., Jr.; Anderson, S.F.; Annis, J.; Bahcall, N.A.; Bakken, J.A.; Barkhouser, R.; Bastian, S.; Berman, E.; et al. The Sloan Digital Sky Survey: Technical Summary. *Astron. J.* **2000**, *120*, 1579.
28. Cracco, V.; Ciroi, S.; Berton, M.; Di Mille, F.; Foschini, L.; La Mura, G.; Rafanelli, P. A spectroscopic analysis of a sample of narrow-line Seyfert 1 galaxies selected from the Sloan Digital Sky Survey. *Mon. Notices R. Astron. Soc.* **2016**, *462*, 1256.
29. Komossa, S.; Voges, W.; Xu, D.; Mathur, S.; Adorf, H.-M.; Lemson, G.; Duschl, W.J.; Grupe, D. Radio-loud Narrow-Line Type 1 Quasars. *Astron. J.* **2006**, *132*, 531.
30. Kellermann, K.I.; Condon, J.J.; Kimball, A.E.; Perley, R.A.; Ivezić, Z. Radio-loud and Radio-quiet QSOs. *Astrophys. J.* **2016**, *831*, 168.
31. Anton, S.; Browne, I.W.A.; Marcha, M.J. The colour of the narrow line Sy1-blazar 0324+3410. *Astron. Astrophys.* **2008**, *490*, 583.

32. Berton, M.; Congiu, E.; Järvela, E.; Antonucci, R.; Kharb, P.; Lister, M.L.; Tarchi, A.; Caccianiga, A.; Chen, S.; Foschini, L.; et al. Radio-emitting narrow-line Seyfert 1 galaxies in the JVLA perspective. *Astron. Astrophys.* **2018**, *614*, A87.
33. Doi, A.; Nagira, H.; Kawakatu, N.; Kino, M.; Nagai, H.; Asada, K. Kiloparsec-scale Radio Structures in Narrow-line Seyfert 1 Galaxies. *Astrophys. J.* **2012**, *760*, 41.
34. Rakshit, S.; Stalin, C.S.; Hota, A.; Konar, C. Rare Finding of a 100 Kpc Large, Double-lobed Radio Galaxy Hosted in the Narrow-line Seyfert 1 Galaxy SDSS J103024.95+551622.7. *Astrophys. J.* **2018**, *869*, 173.
35. Richards, J.; Lister, M.L. Kiloparsec-Scale Jets in Three Radio-Loud Narrow-Line Seyfert 1 Galaxies. *Astrophys. J.* **2015**, *800*, L8.
36. Doi, A.; Asada, K.; Nagai, H. Very Long Baseline Array Imaging of Parsec-scale Jet Structures in Radio-loud Narrow-line Seyfert 1 Galaxies. *Astrophys. J.* **2011**, *738*, 126.
37. Foschini, L.; Maraschi, L.; Tavecchio, F.; Ghisellini, G.; Gliozzi, M.; Sambruna, R.M. Blazar nuclei in radio-loud narrow-line Seyfert 1? *Adv. Space Res.* **2009**, *43*, 889.
38. D'Ammando, F.; Orienti, M.; Finke, J.; Raiteri, C.M.; Angelakis, E.; Fuhrmann, L.; Giroletti, M.; Hovatta, T.; Karamanavis, V.; Max-Moerbeck, W.; et al. Multifrequency studies of the narrow-line Seyfert 1 galaxy SBS 0846+513. *Mon. Notices R. Astron. Soc.* **2013**, *436*, 191.
39. Lister, M.L.; Aller, M.F.; Aller, H.D.; Homan, D.C.; Kellermann, K.I.; Kovalev, Y.Y.; Pushkarev, A.B.; Richards, J.L.; Ros, E.; Savolainen, T. MOJAVE: XIII. Parsec-scale AGN Jet Kinematics Analysis Based on 19 years of VLBA Observations at 15 GHz. *Astron. J.* **2016**, *152*, 12.
40. Deo, R.P.; Crenshaw, D.M.; Kramer, S.B. The Host Galaxies of Narrow-Line Seyfert 1 Galaxies: Nuclear Dust Morphology and Starburst Rings. *Astron. J.* **2006**, *132*, 321.
41. Krongold, Y.; Dultzin-Hacyan, D.; Marziani, P. Host Galaxies and Circumgalactic Environment of "Narrow Line" Seyfert 1 Nuclei. *Astron. J.* **2001**, *121*, 702.
42. Mathur, S.; Fields, D.; Peterson, B.M.; Grupe, D. Supermassive Black Holes, Pseudobulges, and the Narrow-line Seyfert 1 Galaxies. *Astrophys. J.* **2012**, *754*, 146.
43. Ohta, K.; Aoki, K.; Kawaguchi, T.; Kiuchi, G. A Bar Fuels a Supermassive Black Hole?: Host Galaxies of Narrow-Line Seyfert 1 Galaxies. *Astrophys. J. Suppl. Ser.* **2007**, *169*, 1.
44. Orban de Xivry, G.; Davies, R.; Schartmann, M.; Komossa, S.; Marconi, A.; Hicks, E.; Engel, H.; Tacconi, L. The role of secular evolution in the black hole growth of narrow-line Seyfert 1 galaxies. *Mon. Notices R. Astron. Soc.* **2011**, *417*, 2721.
45. Markarian, B.E.; Lipovetsky, V.A.; Stepanian, J.A.; Erastova, L.K.; Shapovalova, A.I. The first Byurakan survey. A catalogue of galaxies with UV-continuum. *Commun. Spec. Astrophys. Obs.* **1989**, *62*, 5.
46. Böttcher, M.; Dermer, C.D. An Evolutionary Scenario for Blazar Unification. *Astrophys. J.* **2002**, *564*, 86.
47. Marscher, A. Jets in AGN. *Lect. Notes Phys.* **2009**, *794*, 173.
48. Sikora, M.; Stawarz, L.; Lasota, J.-P. Radio Loudness of Active Galactic Nuclei: Observational Facts and Theoretical Implications. *Astrophys. J.* **2007**, *658*, 815.
49. Sikora, M. Radio bimodality: Spin, accretion mode, or both? *Astron. Nachr.* **2009**, *330*, 291.
50. Ade, P.A.R.; Aghanim, N.; Arnaud, M.; Ashdown, M.; Aumont, J.; Baccigalupi, C.; Banday, A.J.; Barreiro, R.B.; Bartlett, J.G.; Bartolo, N.; et al. Planck 2015 results XIII. Cosmological parameters. *Astron. Astrophys.* **2016**, *594*, A13.
51. Baldi, R.; Capetti, A.; Robinson, A.; Laor, A.; Behar, E. Radio-loud Narrow Line Seyfert 1 under a different perspective: A revised black hole mass estimate from optical spectropolarimetry. *Mon. Notices R. Astron. Soc.* **2016**, *458*, L69.
52. Gallo, L.C.; Edwards, P.G.; Ferrero, E.; Kataoka, J.; Lewis, D.R.; Ellingsen, S.P.; Misanovic, Z.; Welsh, W.F.; Whiting, M.; Boller, T.; et al. The spectral energy distribution of PKS 2004-447: A compact steep-spectrum source and possible radio-loud narrow-line Seyfert 1 galaxy. *Mon. Notices R. Astron. Soc.* **2006**, *370*, 245.
53. Oshlack, A.Y.K.N.; Webster, R.L.; Whiting, M.T. A Very Radio Loud Narrow-Line Seyfert 1: PKS 2004-447. *Astrophys. J.* **2001**, *558*, 578.

54. Abdo, A.A.; Ackermann, M.; Ajello, M.; Allafort, A.; Antolini, E.; Atwood, W.B.; Axelsson, M.; Baldini, L.; Ballet, J.; Barbiellini, G.; et al. Fermi Large Area Telescope First Source Catalog. *Astrophys. J. Suppl. Ser.* **2010**, *188*, 405.
55. Nolan, P.L.; Abdo, A.A.; Ackermann, M.; Ajello, M.; Allafort, A.; Antolini, E.; Atwood, W.B.; Axelsson, M.; Baldini, L.; Ballet, J.; et al. Fermi Large Area Telescope Second Source Catalog. *Astrophys. J. Suppl. Ser.* **2012**, *199*, 31.
56. D'Ammando, F.; Orienti, M.; Finke, J.; Raiteri, C.M.; Angelakis, E.; Fuhrmann, L.; Giroletti, M.; Hovatta, T.; Max-Moerbeck, W.; Perkins, J.S.; et al. SBS 0846+513: A new  $\gamma$ -ray-emitting narrow-line Seyfert 1 galaxy. *Mon. Notices R. Astron. Soc.* **2012**, *426*, 317.
57. D'Ammando, F.; Orienti, M.; Larsson, J.; Giroletti, M. The first  $\gamma$ -ray detection of the narrow-line Seyfert 1 FBQS J1644+2619. *Mon. Notices R. Astron. Soc.* **2015**, *452*, 520.
58. Atwood, W.B.; Baldini, L.; Bregeon, J.; Bruel, P.; Chekhtman, A.; Cohen-Tanugi, J.; Drlica-Wagner, A.; Granot, J.; Longo, F.; Omodei, N.; et al. New Fermi-LAT Event Reconstruction Reveals More High-energy Gamma Rays from Gamma-Ray Bursts. *Astrophys. J.* **2013**, *774*, 76.
59. Paliya, V.S.; Ajello, M.; Rakshit, S.; Mandal, A.K.; Stalin, C.S.; Kaur, A.; Hartmann, D. Gamma-Ray-emitting Narrow-line Seyfert 1 Galaxies in the Sloan Digital Sky Survey. *Astrophys. J.* **2018**, *853*, L2.
60. Ackermann, M.; Ajello, M.; Atwood, W.B.; Baldini, L.; Ballet, J.; Barbiellini, G.; Bastieri, D.; Becerra Gonzalez, J.; Bellazzini, R.; Bissaldi, E.; et al. The Third Catalog of Active Galactic Nuclei Detected by the Fermi Large Area Telescope. *Astrophys. J. Suppl. Ser.* **2015**, *810*, 14.
61. D'Ammando, F.; Orienti, M.; Finke, J.; Raiteri, C.M.; Hovatta, T.; Larsson, J.; Max-Moerbeck, W.; Perkins, J.; Readhead, A.C.S.; Richards, J.L.; et al. The most powerful flaring activity from the NLSy1 PMN J0948+0022. *Mon. Notices R. Astron. Soc.* **2015**, *446*, 2456.
62. Foschini, L.; Ghisellini, G.; Kovalev, Y.Y.; Lister, M.L.; D'Ammando, F.; Thompson, D.J.; Tramacere, A.; Angelakis, E.; Donato, D.; Falcone, A.; et al. The first gamma-ray outburst of a narrow-line Seyfert 1 galaxy: The case of PMN J0948+0022 in 2010 July. *Mon. Notices R. Astron. Soc.* **2011**, *413*, 1671.
63. D'Ammando, F.; Orienti, M.; Finke, J.; Hovatta, T.; Giroletti, M.; Max-Moerbeck, W.; Pearson, T.J.; Readhead, A.C.S.; Reeves, R.A.; Richards, J.L. The awakening of the  $\gamma$ -ray narrow-Line Seyfert 1 galaxy PKS 1502+036. *Mon. Notices R. Astron. Soc.* **2016**, *463*, 4469.
64. Foschini, L. Evidence of powerful relativistic jets in narrow-line Seyfert 1 galaxies. In *Narrow-Line Seyfert 1 Galaxies and Their Place in the Universe, Proceedings of Science*; Foschini, L., Colpi, M., Gallo, L., Grupe, D., Komossa, S., Leighly, K., Mathur, S., Eds.; SISSA, Trieste **2011**, *NLS1*, 24.
65. Paliya, V.S.; Sahayanathan, S.; Parker, M.L.; Fabian, A.C.; Stalin, C.S.; Anjum, A.; Pandey, S.B. The Peculiar Radio-loud Narrow Line Seyfert 1 Galaxy 1H 0323+342. *Astrophys. J.* **2014**, *789*, 143.
66. Gokus, A. Fermi LAT detection of a GeV flare from the radio-loud narrow-line Seyfert 1 Galaxy PKS 2004-447. *Astron. Telegr.* **2019**, *13229*, 1.
67. Paliya, V.S.; Stalin, C.S. The First GeV Outburst of the Radio-loud Narrow-line Seyfert 1 Galaxy PKS 1502+036. *Astrophys. J.* **2016**, *820*, L52.
68. Abdo, A.A.; Ackermann, M.; Ajello, M.; Atwood, W.B.; Axelsson, M.; Baldini, L.; Ballet, J.; Barbiellini, G.; Bastieri, D.; Bechtol, K.; et al. Spectral Properties of Bright Fermi-Detected Blazars in the Gamma-Ray Band. *Astrophys. J.* **2010**, *710*, 1271.
69. Miller, H.; Maune, J.; Eggen, J.; Turner, C.; Ferrara, E.; Gudkova, D.; Battles, A. A Search for Blazar-Like Radio-Loud Narrow-Line Seyfert 1 Galaxies. *Galaxies* **2015**, *5*, 20.
70. Lähteenmäki, A.; Järvela, E.; Ramakrishnan, V.; Tornikoski, M.; Tammi, J.; Vera, R.J.C.; Chamani, W. Radio jets and gamma-ray emission in radio-silent narrow-line Seyfert 1 galaxies. *Astron. Astrophys.* **2018**, *614*, 1.
71. Paiano, S.; Falomo, R.; Treves, A.; Franceschini, A.; Scarpa, R. Optical Spectroscopic Survey of a Sample of Unidentified Fermi Objects: II. *Astrophys. J.* **2019**, *871*, 162.
72. Kynoch, D.; Landt, H.; Ward, M.J.; Done, C.; Boisson, C.; Baloković, M.; Angelakis, E.; Myserlis, I. The relativistic jet of the  $\gamma$ -ray emitting narrow-line Seyfert 1 galaxy PKS J1222+0413. *Mon. Notices R. Astron. Soc.* **2019**, *487*, 181.

73. Berton, M.; Foschini, L.; Caccianiga, A.; Ciroi, S.; Congiu, E.; Cracco, V.; Frezzato, M.; La Mura, G.; Rafanelli, P. An orientation-based unification of young jetted active galactic nuclei: The case of 3C 286. *Front. Astron. Space Sci.* **2017**, *4*, 8.
74. Liao, M.; Gu, M. Investigation on Young radio AGNs based on SDSS spectroscopy. *Mon. Notices R. Astron. Soc.* **2019**, *in press*.
75. An, T.; Lao, B.-Q.; Zhao, W.; Mohan, P.; Cheng, X.-P.; Cui, Y.-Z.; Zhang, Z.-L. Parsec-scale jet properties of the gamma-ray quasar 3C 286. *Mon. Notices R. Astron. Soc.* **2017**, *466*, 952.
76. Ajello, M.; Atwood, W.B.; Baldini, L.; Ballet, J.; Barbiellini, G.; Bastieri, D.; Bellazzini, R.; Bissaldi, E.; Blandford, R.D.; Bloom, E.D.; et al. 3FHL: The Third Catalog of Hard Fermi-LAT Sources. *Astrophys. J. Suppl. Ser.* **2017**, *232*, 18.
77. Ackermann, M.; Ajello, M.; Atwood, W.B.; Baldini, L.; Ballet, J.; Barbiellini, G.; Bastieri, D.; Becerra Gonzalez, J.; Bellazzini, R.; Bissaldi, E.; et al. 2FHL: The Second Catalog of Hard Fermi-LAT Sources. *Astrophys. J. Suppl. Ser.* **2016**, *222*, 5.
78. Falcone, A.D.; Bond, I.H.; Boyle, P.J.; Bradbury, S.M.; Buckley, J.H.; Carter-Lewis, D.; Celik, O.; Cui, W.; Daniel, M.; D'Vali, M.; et al. A Search for TeV Gamma-Ray Emission from High-peaked Flat-Spectrum Radio Quasars Using the Whipple Air Cerenkov Telescope. *Astrophys. J.* **2004**, *613*, 710.
79. Archambault, S.; Archer, A.; Benbow, W.; Bird, R.; Biteau, J.; Buchovecky, M.; Buckley, J.H.; Bugaev, V.; Byrum, K.; Cerruti, M.; et al. Upper Limits from Five Years of Blazar Observations with the VERITAS Cherenkov Telescopes. *Astron. J.* **2016**, *151*, 142.
80. Abramowski, A.; Aharonian, F.; Ait Benkhali, F.; Akhperjanian, A.G.; Angüner, E.; Anton, G.; Balenderan, S.; Balzer, A.; Barnacka, A.; Becherini, Y.; et al. Flux upper limits for 47 AGN observed with H.E.S.S. in 2004–2011. *Astron. Astrophys.* **2014**, *564*, A9.
81. Ahnen, M.L.; Ansoldi, S.; Antonelli, L.A.; Antoranz, P.; Arcaro, C.; Babic, A.; Banerjee, B.; Bangale, P.; Barres de Almeida, U.; Barrio, J.A.; et al. Detection of very high energy gamma-ray emission from the gravitationally lensed blazar QSO B0218+357 with the MAGIC telescopes. *Astron. Astrophys.* **2016**, *595*, A98.
82. Abeysekara, A.U.; Archambault, S.; Archer, A.; Aune, T.; Barnacka, A.; Benbow, W.; Bird, R.; Biteau, J.; Buckley, J.H.; Bugaev, V.; et al. Gamma-Rays from the Quasar PKS 1441+25: Story of an Escape. *Astrophys. J. Lett.* **2015**, *815*, L22.
83. Ahnen, M.L.; Ansoldi, S.; Antonelli, L.A.; Antoranz, P.; Babic, A.; Banerjee, B.; Bangale, P.; Barres de Almeida, U.; Barrio, J.A.; Bednarek, W.; et al. Very High Energy  $\gamma$ -Rays from the Universe's Middle Age: Detection of the  $z = 0.940$  Blazar PKS 1441+25 with MAGIC. *Astrophys. J. Lett.* **2015**, *815*, L23.
84. Mirzoyan, R. Detection of very-high-energy gamma-ray emission from the FSRQ Ton 0599 with the MAGIC telescopes. *Astron. Telegr.* **2017**, *11061*, 1.
85. Costamante, L.; Cutini, S.; Tosti, G.; Antolini, E.; Tramacere, A. On the origin of gamma-rays in Fermi blazars: Beyond the broad-line region. *Mon. Notices R. Astron. Soc.* **2018**, *477*, 4477.
86. Tavecchio, F.; Ghisellini, G. "Flat" broad line region and gamma-ray absorption in blazars. *arXiv* **2012**, arXiv:1209.2291.
87. Albert, J.; Aliu, E.; Anderhub, H.; Antonelli, L.A.; Antoranz, P.; Backes, M.; Baixeras, C.; Barrio, J.A.; Bartko, H.; Bastieri, D.; et al. Very-High-Energy gamma rays from a Distant Quasar: How Transparent Is the Universe? *Science* **2008**, *320*, 1752.
88. Aleksić, J.; Antonelli, L.A.; Antoranz, P.; Backes, M.; Barrio, J.A.; Bastieri, D.; Becerra González, J.; Bednarek, W.; Berdyugin, A.; Berger, K.; et al. MAGIC Discovery of Very High Energy Emission from the FSRQ PKS 1222+21. *Astrophys. J.* **2011**, *730*, L8.
89. Aleksić, J.; Antonelli, L.A.; Antoranz, P.; Backes, M.; Barrio, J.A.; Bastieri, D.; Becerra González, J.; Bednarek, W.; Berdyugin, A.; Berger, K.; et al. MAGIC Observations and multiwavelength properties of the quasar 3C 279 in 2007 and 2009. *Astron. Astrophys.* **2011**, *530*, A4.
90. Abramowski, A.; Acero, F.; Aharonian, F.; Akhperjanian, A.G.; Anton, G.; Balenderan, S.; Balzer, A.; Barnacka, A.; Becherini, Y.; Becker, T.; et al. H.E.S.S. discovery of VHE  $\gamma$ -rays from the quasar PKS 1510-089. *Astron. Astrophys.* **2013**, *554*, A107.

91. Aleksić, J.; Ansoldi, S.; Antonelli, L.A.; Antoranz, P.; Babic, A.; Bangale, P.; Barres de Almeida, U.; Barrio, J.A.; Becerra González, J.; Bednarek, W.; et al. MAGIC gamma-ray and multi-frequency observations of flat spectrum radio quasar PKS 1510-089 in early 2012. *Astron. Astrophys.* **2014**, *569*, A46.
92. Mukherjee, R. VERITAS Detection of VHE Emission from Ton 599. *Astron. Telegr.* **2017**, *11075*, 1.
93. Finke, J.D.; Razzaque, S.; Dermer, C.D. Modeling the Extragalactic Background Light from Stars and Dust. *Astrophys. J.* **2010**, *712*, 238.
94. Acharya, B.S.; Agudo, I.; Al Samarai, I.; Alfaro, R.; Alfaro, J.; Alispach, C.; AlvesBatista, R.; Amans, J.-P.; Amato, E.; Ambrosi, G.; et al. Science with the Cherenkov Telescope Array. *World Sci.* **2019**, DOI: 10.1142/10986.
95. Meyer, E.; Finke, J.; Younes, G.; D'Ammando, F.; Rani, B.; Buson, S.; Wadiasingh, Z.; Agudo, I.; Beckmann, V.; Longo, F. Prospects for AGN Studies at Hard X-ray through MeV Energies. *arXiv* **2019**, arXiv:1903.07553.
96. Romano, P.; Vercellone, S.; Foschini, L.; Tavecchio, F.; Landoni, M.; Knödseder, J. Prospects for gamma-ray observations of narrow-line Seyfert 1 galaxies with the Cherenkov Telescope Array. *Mon. Notices R. Astron. Soc.* **2018**, *481*, 5046.
97. D'Ammando, F.; Larsson, J.; Orienti, M.; Torresi, E.; Finke, J. The XMM-Newton view of  $\gamma$ -ray emitting narrow-line Seyfert 1 galaxies. In Proceedings of the X-Ray Universe 2017, Rome, Italy, 6–9 June 2017.
98. Kynoch, D.; Landt, H.; Ward, M.J.; Done, C.; Gardner, E.; Boisson, C.; Arrieta-Lobo, M.; Zech, A.; Steenbrugge, K.; Pereira Santaella, M. The relativistic jet of the  $\gamma$ -ray emitting narrow-line Seyfert 1 galaxy 1H 0323+342. *Mon. Notices R. Astron. Soc.* **2018**, *475*, 404.
99. Larsson, J.; D'Ammando, F.; Falocco, S.; Giroletti, M.; Orienti, M.; Piconcelli, E.; Righini, S. FBQS J1644+2619: Multiwavelength properties and its place in the class of  $\gamma$ -ray emitting Narrow Line Seyfert 1s. *Mon. Notices R. Astron. Soc.* **2018**, *476*, 43.
100. Yang, H.; Yuan, W.; Yao, S.; Li Y.; Zhang, J.; Zhou, H.; Komossa, S.; Liu, H.-Y.; Jin, C. SDSS J211852.96-073227.5: A new  $\gamma$ -ray flaring narrow-line Seyfert 1 galaxy. *Mon. Notices R. Astron. Soc.* **2018**, *477*, 5127.
101. Kreikenbohm, A.; Schulz, R.; Kadler, M.; Wilms, J.; Markowitz, A.; Chang, C.S.; Carpenter, B.; Elsässer, D.; Gehrels, N.; Mannheim, K.; et al. The gamma-ray emitting radio-loud narrow-line Seyfert 1 galaxy PKS 2004-447. I. The X-ray View. *Astron. Astrophys.* **2016**, *585*, 91.
102. Orienti, M.; D'Ammando, F.; Larsson, J.; Finke, J.; Giroletti, M.; Dallacasa, D.; Isacson, T.; Stoby Hoglund, J. Investigating powerful jets in radio-loud narrow-line Seyfert 1s. *Mon. Notices R. Astron. Soc.* **2015**, *453*, 4037.
103. D'Ammando, F.; Larsson, J.; Orienti, M.; Raiteri, C.M.; Angelakis, E.; Carraminana, A.; Carrasco, L.; Drake, A.J.; Fuhrmann, L.; Giroletti, M.; et al. Multiwavelength observations of the  $\gamma$ -ray-emitting narrow-line Seyfert 1 PMN J0948+0022 in 2011. *Mon. Notices R. Astron. Soc.* **2014**, *438*, 3521
104. Gierlinski, M.; Done, C. Is the soft excess in active galactic nuclei real? *Mon. Notices R. Astron. Soc.* **2004**, *349*, L7.
105. Kataoka, J.; Madejski, G.; Sikora, M.; Roming, P.; Chester, M.M.; Grupe, D.; Tsubuku, Y.; Sato, R.; Kawai, N.; Tosti, G.; et al. Multiwavelength Observations of the Powerful Gamma-Ray Quasar PKS 1510-089: Clues on the Jet Composition. *Astrophys. J.* **2008**, *672*, 787.
106. Grandi, P.; Palumbo, G. Jet and Accretion-Disk Emission Untangled in 3C 273. *Science* **2004**, *303*, 998.
107. De Rosa, A.; Bassani, L.; Ubertini, P.; Malizia, A.; Dean, A.J. Bulk Compton motion in the luminous quasar 4C04.42? *Mon. Notices R. Astron. Soc.* **2008**, *388*, L54.
108. Celotti, A.; Ghisellini, G.; Fabian, A.C. Bulk Comptonization spectra in blazars. *Mon. Notices R. Astron. Soc.* **2007**, *375*, 417.
109. Barcons, X.; Barret, D.; Decourchelle, A.; den Herder, J.W.; Fabian, A.C.; Matsumoto, H.; Lumb, D.; Nandra, K.; Piro, L.; Smith, R.K.; Willingale, R. Athena: ESA's X-ray observatory for the late 2020s. *Astron. Nachr.* **2017**, *338*, 153.
110. In't Zand, J.M.; Bozzo, E.; Qu, J.; Li, X.-D.; Amati, L.; Chen, Y.; Donnarumma, I.; Doroshenko, V.; Drake, S.A.; Hernanz, M.; et al. Observatory science with eXTP. *Sci. China Phys. Mech. Astron.* **2019**, *62*, 29506.
111. Tashiro, M.; Maejima, H.; Toda, K.; Kelley, R.; Reichenthal, L.; Lobell, J.; Petre, R.; Guainazzi, M.; Costantini, E.; Edison, M.; et al. Concept of the X-ray Astronomy Recovery Mission. *SPIE* **2018**, *10699*, 22.
112. D'Ammando, F.; Gokus, A.; Kadler, M.; Ojha, R. Swift follow-up of the flaring NLSy1 PKS 2004-447. *Astron. Telegr.* **2019**, *13233*, 1.

113. Boller, T.; Brandt, W.N.; Fabian, A.C.; Fink, H. ROSAT monitoring of persistent giant and rapid variability in the narrow-line Seyfert 1 galaxy IRAS 13224-3809. *Mon. Notices R. Astron. Soc.* **1997**, *289*, 393.
114. D'Ammando, F.; Rau, A.; Schady, P.; Finke, J.; Orienti, M.; Greiner, J.; Kann, D.A.; Ojha, R.; Foley, A.R.; Stevens, J.; et al. PKS 2123-463: A confirmed  $\gamma$ -ray blazar at high redshift. *Mon. Notices R. Astron. Soc.* **2012**, *427*, 893.
115. Raiteri, C.M.; Villata, M.; Smith, P.S.; Larionov, V.M.; Acosta-Pulido, J.A.; Aller, M.F.; D'Ammando, F.; Gurwell, M.A.; Jorstad, S.G.; Joshi, M.; et al. Variability of the blazar 4C 38.41 (B3 1633+382) from GHz frequencies to GeV energies. *Astron. Astrophys.* **2012**, *545*, A48.
116. Wehrle, A.E.; Marscher, A.P.; Jorstad, S.G.; Gurwell, M.A.; Manasvita, J.; MacDonald, N.R.; Williamson, K.E.; Agudo, I.; Grupe, D. Multiwavelength variations of 3C 454.3 during the 2010 November to 2011 January Outburst. *Astrophys. J.* **2012**, *758*, 72.
117. Oh, K.; Koss, M.; Markwardt, C.B.; Schawinski, K.; Baumgartner, W.H.; Barthelmy, S.D.; Cenko, S.B.; Gehrels, N.; Mushotzky, R.; Petulante, A.; et al. The 105-Month Swift-BAT All-sky Hard X-Ray Survey. *Astrophys. J. Suppl. Ser.* **2018**, *235*, 4.
118. Bird, A.J.; Bazzano, A.; Bassani, L.; Capitanio, F.; Fiacchi, M.; Hill, A.B.; Malizia, A.; McBride, V.A.; Scaringi, S.; Sguera, V.; et al. The Fourth IBIS/ISGRI Soft Gamma-ray Survey Catalog. *Astrophys. J. Suppl. Ser.* **2010**, *186*, 1.
119. Brenneman, L. Illuminating the Disk/Corona/Jet Connection in NLS1 Galaxies. In Proceedings of the X-Ray Universe 2017, Rome, Italy, 6–9 June 2017.
120. Landt, H.; Ward, M.J.; Baloković, M.; Kynoch, D.; Storchi-Bergmann, T.; Boisson, C.; Done, C.; Schimoia, J.; Stern, D. On the black hole mass of the  $\gamma$ -ray emitting narrow-line Seyfert 1 galaxy 1H 0323+342. *Mon. Notices R. Astron. Soc.* **2017**, *464*, 2565.
121. D'Ammando, F.; Acosta-Pulido, J.A.; Capetti, A.; Raiteri, C.M.; Baldi, R.D.; Orienti, M.; Ramos Almeida, C. Uncovering the host galaxy of the  $\gamma$ -ray-emitting narrow-line Seyfert 1 galaxy FBQS J1644+2619. *Mon. Notices R. Astron. Soc.* **2017**, *469*, L11.
122. Caccianiga, A.; Antón, S.; Ballo, L.; Foschini, L.; Maccacaro, T.; Della Ceca, R.; Severgnini, P.; Marchã, M.J.; Mateos, S.; Sani, E. WISE colours and star formation in the host galaxies of radio-loud narrow-line Seyfert 1. *Mon. Notices R. Astron. Soc.* **2015**, *451*, 1795.
123. Jiang, N.; Zhou, H.-Y.; Ho, L.C.; Yuan, W.; Wang, T.-G.; Dong, X.-B.; Jiang, P.; Ji, T.; Tian, Q. Rapid Infrared Variability of Three Radio-loud Narrow-line Seyfert 1 Galaxies: A View from the Wide-field Infrared Survey Explorer. *Astrophys. J.* **2012**, *759*, L31.
124. Itoh, R.; Tanaka, Y.T.; Fukazawa, Y.; Kawabata, K.S.; Kawaguchi, K.; Moritani, Y.; Takaki, K.; Ueno, I.; Uemura, M.; Akitaya, H.; et al. Minute-scale Rapid Variability of the Optical Polarization in the Narrow-line Seyfert 1 Galaxy PMN J0948+0022. *Astrophys. J.* **2013**, *775*, L26.
125. Liu, H.; Wang, J.; Mao, Y.; Wei, J. Violent Intranight Optical Variability of a Radio-loud Narrow-line Seyfert 1 Galaxy: SDSS J094857.3+002225. *Astrophys. J.* **2010**, *715*, L113.
126. Maune, J.D.; Miller, H.R.; Eggen, J.R. The Extreme Optical Variability of J0948+0022. *Astrophys. J.* **2013**, *762*, 124.
127. Paliya, V.S.; Stalin, C.S.; Kumar, B.; Kumar, B.; Bhatt, V.K.; Pandey, S.B.; Yadav, R.K.S. Intranight optical variability of  $\gamma$ -ray-loud narrow-line Seyfert 1 galaxies. *Mon. Notices R. Astron. Soc.* **2013**, *428*, 2450.
128. Maune, J.D.; Eggen, J.R.; Miller, H.R.; Marshall, K.; Readhead, A.C.S.; Hovatta, T.; King, O. The Extreme Behavior of the Radio-loud Narrow-line Seyfert 1 Galaxy J0849+5108. *Astrophys. J.* **2014**, *794*, 93.
129. Paliya, V.S.; Rajput, B.; Stalin, C.S.; Pandey, S.B. Broadband Observations of the Gamma-Ray Emitting Narrow Line Seyfert 1 Galaxy SBS 0846+513. *Astrophys. J.* **2016**, *819*, 121.
130. Itoh, R.; Tanaka, Y.T.; Akitaya, H.; Uemura, M.; Fukazawa, Y.; Inoue, Y.; Doi, A.; Arai, A.; Hanayama, H.; Hashimoto, O.; et al. Variable optical polarization during high state in  $\gamma$ -ray loud, narrow-line Seyfert 1 galaxy 1H 0323+342. *Publ. Astron. Soc. Jpn.* **2014**, *66*, 108.
131. Ojha, V.; Krishna, G.; Chand, H. Intra-night optical monitoring of three  $\gamma$ -ray detected narrow-line Seyfert 1 galaxies. *Mon. Notices R. Astron. Soc.* **2019**, *483*, 3036.
132. Angelakis, E.; Kiehlmann, S.; Myserlis, I.; Blinov, D.; Eggen, J.; Itoh, R.; Marchili, N.; Zensus, J.A. Optical polarisation variability of radio-loud narrow-line Seyfert 1 galaxies. Search for long rotations of the polarisation plane. *Astron. Astrophys.* **2018**, *618*, A92.

133. Angelakis, E.; Hovatta, T.; Blinov, D.; Pavlidou, V.; Kiehlmann, S.; Myserlis, I.; Böttcher, M.; Mao, P.; Panopoulou, G.V.; Liodakis, I.; et al. RoboPol: The optical polarization of gamma-ray-loud and gamma-ray-quiet blazars. *Mon. Notices R. Astron. Soc.* **2016**, *463*, 3365.
134. Abdo, A.A.; Ackermann, M.; Ajello, M.; Axelsson, M.; Baldini, L.; Ballet, J.; Barbiellini, G.; Bastieri, D.; Baughman, B.M.; Bechtol, K.; et al. A change in the optical polarization associated with a  $\gamma$ -ray flare in the blazar 3C 279. *Nature* **2010**, *463*, 919.
135. Blinov, D.; Pavlidou, V.; Papadakis, I.E.; Hovatta, T.; Pearson, T.J.; Liodakis, I.; Panopoulou, G.V.; Angelakis, E.; Baloković, M.; Das, H.; et al. RoboPol: Optical polarization-plane rotations and flaring activity in blazars. *Mon. Notices R. Astron. Soc.* **2016**, *457*, 2252.
136. Blinov, D.; Pavlidou, V.; Papadakis, I.; Kiehlmann, S.; Liodakis, I.; Panopoulou, G.V.; Angelakis, E.; Baloković, M.; Hovatta, T.; King, O.G.; et al. RoboPol: Connection between optical polarization plane rotations and gamma-ray flares in blazars. *Mon. Notices R. Astron. Soc.* **2018**, *474*, 1296.
137. Marscher, A.P.; Jorstad, S.G.; D’Arcangelo, F.D.; Smith, P.S.; Williams, G.G.; Larionov, V.M.; Oh, H.; Olmstead, A.R.; Aller, M.F.; Aller, H.D.; et al. The inner jet of an active galactic nucleus as revealed by a radio-to- $\gamma$ -ray outburst. *Nature* **2008**, *452*, 966.
138. Marscher, A.P. Turbulent, Extreme Multi-zone Model for Simulating Flux and Polarization Variability in Blazars. *Astrophys. J.* **2014**, *780*, 87.
139. Zhang, H.; Chen, X.; Böttcher, M. Synchrotron Polarization in Blazars. *Astrophys. J.* **2014**, *789*, 66.
140. Marscher, A.; Jorstad, S.; Williamson, K. Modeling the Time-Dependent Polarization of Blazars. *Galaxies* **2017**, *5*, 63.
141. Ghisellini, G.; Tavecchio, F.; Foschini, L.; Ghirlanda, G. The transition between BL Lac objects and flat spectrum radio quasars. *Mon. Notices R. Astron. Soc.* **2011**, *414*, 2674.
142. Orienti, M.; D’Ammando, F.; Giroletti, M. High resolution radio observations of gamma-ray emitting Narrow-Line Seyfert 1s. In Proceedings of 2011 Fermi & Jansky: Our Evolving Understanding of AGN, St Michaels, MD, USA, 10–12 November 2011.
143. Hada, K.; Doi, A.; Wajima, K.; D’Ammando, F.; Orienti, M.; Giroletti, M.; Giovannini, G.; Nakamura, M.; Asada, K. Collimation, Acceleration, and Recollimation Shock in the Jet of Gamma-Ray Emitting Radio-loud Narrow-line Seyfert 1 Galaxy 1H0323+342. *Astrophys. J.* **2018**, *860*, 141.
144. Wajima, K.; Fujisawa, K.; Hayashida, M.; Isobe, N.; Ishida, T.; Yonekura, Y. Short-term Radio Variability and Parsec-scale Structure in a Gamma-Ray Narrow-line Seyfert 1 Galaxy 1H 0323+342. *Astrophys. J.* **2014**, *781*, 75.
145. Doi, A.; Fujisawa, K.; Inoue, M.; Wajima, K.; Nagai, H.; Harada, K.; Suematsu, K.; Habe, A.; Honma, M.; Kawaguchi, N.; et al. Japanese VLBI Network Observations of Radio-Loud Narrow-Line Seyfert 1 Galaxies. *Publ. Astron. Soc. Jpn.* **2007**, *59*, 703.
146. Gu, M.; Chen, Y.; Komossa, S.; Yuan, W.; Shen, Z.; Wajima, K.; Zhou, H.; Zensus, J.A. The Radio Properties of Radio-loud Narrow-line Seyfert 1 Galaxies on Parsec Scales. *Astrophys. J. Suppl. Ser.* **2015**, *221*, 3.
147. D’Ammando, F.; Orienti, M.; Doi, A.; Giroletti, M.; Dallacasa, D.; Hovatta, T.; Drake, A.J.; Max-Moerbeck, W.; Readhead, A.C.S.; Richards, J.L. The ordinary life of the  $\gamma$ -ray emitting narrow-line Seyfert 1 galaxy PKS 1502+036. *Mon. Notices R. Astron. Soc.* **2013**, *433*, 952.
148. Giroletti, M.; Paragi, Z.; Bignall, H.; Doi, A.; Foschini, L.; Gabányi, K.É.; Reynolds, C.; Blanchard, J.; Campbell, R.M.; Colomer, F.; et al. Global e-VLBI observations of the gamma-ray narrow line Seyfert 1 PMN J0948+0022. *Astron. Astrophys.* **2011**, *528*, L11.
149. Doi, A.; Nakahara, S.; Nakamura, M.; Kino, M.; Kawakatu, N.; Nagai, H. Radio jet structures at 100 pc and larger scales of the  $\gamma$ -ray-emitting narrow-line Seyfert 1 galaxy PMN J0948+0022. *Mon. Notices R. Astron. Soc.* **2019**, *487*, 640.
150. Caccianiga, A.; Anton, S.; Ballo, L.; Dallacasa, D.; Della Ceca, R.; Fanali, R.; Foschini, L.; Hamilton, T.; Kraus, A.; Maccararo, T.; et al. SDSS J143244.91+301435.3: A link between radio-loud narrow-line Seyfert 1 galaxies and compact steep-spectrum radio sources? *Mon. Notices R. Astron. Soc.* **2014**, *442*, 171.
151. Tengstrand, O.; Guainazzi, M.; Siemiginowska, A.; Fonseca Bonilla, N.; Labiano, A.; Worrall, D.M.; Grandi, P.; Piconcelli, E. The X-ray view of giga-hertz peaked spectrum radio galaxies. *Astron. Astrophys.* **2009**, *501*, 89.

152. Doi, A.; Hada, K.; Kino, M.; Wajima, K.; Nakahara, S. A Recollimation Shock in a Stationary Jet Feature with Limb-brightening in the Gamma-Ray-emitting Narrow-line Seyfert 1 Galaxy 1H 0323+342. *Astrophys. J. Lett.* **2018**, *857*, L6.
153. Lister, M.L.; Homan, D.C.; Hovatta, T.; Kellermann, K.I.; Kiehlmann, S.; Kovalev, Y.Y.; Max-Moerbeck, W.; Pushkarev, A.B.; Readhead, A.C.S.; Ros, E.; et al. MOJAVE. XVII. Jet Kinematics and Parent Population Properties of Relativistically Beamed Radio-loud Blazars. *Astrophys. J.* **2019**, *874*, 43.
154. Piner, B.G.; Edwards, P.G. The Parsec-Scale Structure and Jet Motions of the TeV Blazars 1ES 1959+650, PKS 2155-304, and 1ES 2344+514. *Astrophys. J.* **2004**, *600*, 115.
155. Piner, B.G.; Pant, N.; Edwards, P.G. The Jets of TeV Blazars at Higher Resolution: 43 GHz and Polarimetric VLBA Observations from 2005 to 2009. *Astrophys. J.* **2010**, *723*, 1150.
156. Piner, B.G.; Edwards, P.G. The Doppler crisis in TeV blazars and its possible resolutions. In *Fourteenth Marcel Grossmann Meet. Recent Dev. Theor. Exp. Gen. Relativ. Astrophys. Relativ. Field Theor.; World Sci.; Bianchi, M., Jansen, R. T., Ruffini, R., Eds., 2018*; 3074.
157. Hodge, M.A.; Lister, M.L.; Aller, M.F.; Aller, H.D.; Kovalev, Y.Y.; Pushkarev, A.B.; Savolainen, T. MOJAVE XVI: Multiepoch Linear Polarization Properties of Parsec-scale AGN Jet Cores. *Astrophys. J.* **2018**, *862*, 151.
158. Cheung, C.C.; Harris, D.E.; Stawarz, L. Superluminal Radio Features in the M87 Jet and the Site of Flaring TeV Gamma-Ray Emission. *Astrophys. J. Lett.* **2007**, *663*, L65.
159. Agudo, I.; Jorstad, S.G.; Marscher, A.P.; Larionov, V.M.; Gomez, J.L.; Lähteenmäki, A.; Gurwell, M.; Smith, P.S.; Wiesemeyer, H.; Thum, C.; et al. Location of  $\gamma$ -ray Flare Emission in the Jet of the BL Lacertae Object OJ 287 More than 14 pc from the Central Engine. *Astrophys. J.* **2011**, *726*, L13.
160. Marscher, A.P.; Jorstad, S.G.; Larionov, V.M.; Aller, M.F.; Aller, H.D.; Lähteenmäki, A.; Agudo, I.; Smith, P.S.; Gurwell, M.; Hagen-Thorn, V.A.; et al. Probing the Inner Jet of the Quasar PKS 1510-089 with Multi-Waveband Monitoring During Strong Gamma-Ray Activity. *Astrophys. J.* **2010**, *710*, L126.
161. Orienti, M.; Koyama, S.; D'Ammando, F.; Giroletti, M.; Kino, M.; Nagai, H.; Venturi, T.; Dallacasa, D.; Giovannini, G.; Angelakis, E.; et al. Radio and  $\gamma$ -ray follow-up of the exceptionally high-activity state of PKS 1510-089 in 2011. *Mon. Notices R. Astron. Soc.* **2013**, *428*, 2418.
162. Readhead, A.C.S. Equipartition brightness temperature and the inverse Compton catastrophe. *Astrophys. J.* **1994**, *426*, 51.
163. Angelakis, E.; Fuhrmann, L.; Marchili, N.; Foschini, L.; Myserlis, I.; Karamanavis, V.; Komossa, S.; Blinov, D.; Krichbaum, T.P.; Sievers, A.; et al. Radio jet emission from GeV-emitting narrow-line Seyfert 1 galaxies. *Astron. Astrophys.* **2015**, *575*, A55.
164. D'Ammando, F.; Antolini, E.; Tosti, G.; Finke, J.; Ciprini, S.; Larsson, S.; Ajello, M.; Covino, S.; Gasparrini, D.; Gurwell, M.; et al. Long-term monitoring of PKS 0537-441 with Fermi-LAT and multiwavelength observations. *Mon. Notices R. Astron. Soc.* **2013**, *431*, 2481.
165. Chatterjee, R.; Nalewajko, K.; Myers, A.D. Implications of the Anomalous Outburst in the Blazar PKS 0208-512. *Mon. Notices R. Astron. Soc.* **2013**, *771*, L25.
166. D'Ammando, F.; Raiteri, C.M.; Villata, M.; Romano, P.; Pucella, G.; Krimm, H.A.; Covino, S.; Orienti, M.; Giovannini, G.; Vercellone, S.; et al. AGILE detection of extreme  $\gamma$ -ray activity from the blazar PKS 1510-089 during March 2009. Multifrequency analysis. *Astron. Astrophys.* **2011**, *529*, 145.
167. Raiteri, C.M.; Villata, M.; Acosta-Pulido, J.A.; Agudo, I.; Arkharov, A.A.; Bachev, R.; Baida, G.V.; Benítez, E.; Borman, G.A.; Boschin, W.; et al. Blazar spectral variability as explained by a twisted inhomogeneous jet. *Nature* **2017**, *552*, 374.
168. Dutka, M.S.; Ojha, R.; Pottschmidt, K.; Finke, J.D.; Stevens, J.; Edwards, P.G.; Blanchard, J.; Lovell, J.E.J.; Nesci, R.; Kadler, M.; et al. Multi-wavelength Observations of PKS 2142-75 during Active and Quiescent Gamma-Ray States. *Astrophys. J.* **2013**, *779*, 174.
169. Buson, S.; Longo, F.; Larsson, S.; Cutini, S.; Finke, J.; Ciprini, S.; Ojha, R.; D'Ammando, F.; Donato, D.; Thompson, D.J.; et al. Unusual flaring activity in the blazar PKS 1424-418 during 2008-2011. *Astron. Astrophys.* **2014**, *569*, A40.
170. Finke, J. Compton Dominance and the Blazar Sequence. *Astrophys. J.* **2013**, *763*, 134.

171. Foschini, L.; Berton, M.; Caccianiga, A.; Ciroi, S.; Cracco, V.; Peterson, B.M.; Angelakis, E.; Braitto, V.; Fuhrmann, L.; Gallo, L.; et al. Properties of flat-spectrum radio-loud narrow-line Seyfert 1 galaxies. *Astron. Astrophys.* **2015**, *575*, A13.
172. Chiaberge, M.; Marconi, A. On the origin of radio loudness in active galactic nuclei and its relationship with the properties of the central supermassive black hole. *Mon. Notices R. Astron. Soc.* **2011**, *416*, 917.
173. Ghisellini, G.; Tavecchio, F.; Maraschi, L.; Celotti, A.; Sbarrato, T. The power of relativistic jets is larger than the luminosity of their accretion disks. *Nature* **2014**, *515*, 376.
174. Chiaberge, M.; Gilli, R.; Lotz, J.M.; Norman, C. Radio Loud AGNs are Mergers. *Astrophys. J.* **2015**, *806*, 147.
175. Ramos Almeida, C.; Tadhunter, C.N.; Inskip, K.J.; Morganti, R.; Holt, J.; Dicken, D. The optical morphologies of the 2 Jy sample of radio galaxies: Evidence for galaxy interactions. *Mon. Notices R. Astron. Soc.* **2011**, *410*, 155.
176. Bentz, M.C.; Katz, S. The AGN Black Hole Mass Database. *Publ. Astron. Soc. Pac.* **2015**, *127*, 67.
177. Calderone, G.; Ghisellini, G.; Colpi, M.; Dotti, M. Black hole mass estimate for a sample of radio-loud narrow-line Seyfert 1 galaxies. *Mon. Notices R. Astron. Soc.* **2013**, *431*, 210.
178. Calderone, G.; D'Ammando, F.; Sbarrato, T. The Mass of RL-NLS1 Black Holes: Reconciling Accretion Disk and Virial Estimates. In Proceedings of the Science 2018, "Revisiting Narrow-Line Seyfert 1 Galaxies and Their Place in the Universe" Conference, Padova, 9-13 April 2018, **2018**; 44.
179. D'Ammando, F.; Acosta-Pulido, J.A.; Capetti, A.; Baldi, R.D.; Orienti, M.; Raiteri, C.M.; Ramos Almeida, C. The host galaxy of the  $\gamma$ -ray-emitting narrow-line Seyfert 1 galaxy PKS 1502+036. *Mon. Notices R. Astron. Soc.* **2018**, *478*, L66.
180. Kaspi, S.; Maoz, D.; Netzer, H.; Peterson, B.M.; Vestergaard, M.; Jannuzi, B.T. The Relationship between Luminosity and Broad-Line Region Size in Active Galactic Nuclei. *Astrophys. J.* **2005**, *629*, 61.
181. Leon Tavares, J.; Kotilainen, J.; Chavushyan, V.; Anorve, C.; Puerari, I.; Cruz-González, I.; Patino-Alvarez, V.; Antón, S.; Carraminana, A.; Carrasco, L.; et al. The Host Galaxy of the Gamma-Ray Narrow-line Seyfert 1 Galaxy 1H 0323+342. *Astrophys. J.* **2014**, *795*, 58.
182. Atkinson, J.W.; Collett, J.L.; Marconi, A.; Axon, D.J.; Alonso-Herrero, A.; Batcheldor, D.; Binney, J.J.; Capetti, A.; Carollo, C.M.; Dressel, L.; et al. Supermassive black hole mass measurements for NGC 1300 and 2748 based on Hubble Space Telescope emission-line gas kinematics. *Mon. Notices R. Astron. Soc.* **2005**, *359*, 504.
183. Pastorini, G.; Marconi, A.; Capetti, A.; Axon, D.J.; Alonso-Herrero, A.; Atkinson, J.; Batcheldor, D.; Carollo, C.M.; Collett, J.; Dressel, L.; et al. Supermassive black holes in the Sbc spiral galaxies NGC 3310, NGC 4303 and NGC 4258. *Astron. Astrophys.* **2007**, *469*, 405.
184. Crenshaw, D.M.; Kraemer, S.B.; Gabel, J.R. The Host Galaxies of Narrow-Line Seyfert 1 Galaxies: Evidence for Bar-Driven Fueling. *Astron. J.* **2003**, *126*, 1690.
185. Zhou, H.; Wang, T.; Yuan, W.; Shan, H.; Komossa, S.; Lu, H.; Liu, Y.; Xu, D.; Bai, J.M.; Jiang, D.R. A Narrow-Line Seyfert 1-Blazar Composite Nucleus in 2MASX J0324+3410. *Astrophys. J.* **2007**, *658*, L13.
186. Kotilainen, J.K.; León-Tavares, J.; Olguín-Iglesias, A.; Baes, M.; Anórve, C.; Chavushyan, V.; Carrasco, L. Discovery of a Pseudobulge Galaxy Launching Powerful Relativistic Jets. *Astrophys. J.* **2016**, *832*, 157.
187. Olguin-Iglesias, A.; Kotilainen, J.K.; Leon Tavares, J.; Chavushyan, V.; Anorve, C. Evidence of bar-driven secular evolution in the gamma-ray narrow-line Seyfert 1 galaxy FBQS J164442.5+261913. *Mon. Notices R. Astron. Soc.* **2017**, *467*, 3712.
188. Marconi, A.; Hunt, L. The Relation between Black Hole Mass, Bulge Mass, and Near-Infrared Luminosity. *Astrophys. J.* **2003**, *589*, L21.
189. Einasto, M.; Lietzen, H.; Tempel, E.; Gramann, M.; Liivamägi, L.J.; Einasto, J. SDSS superclusters: Morphology and galaxy content. *Astron. Astrophys.* **2014**, *562*, A87.
190. Kuutma, T.; Tamm, A.; Tempel, E. From voids to filaments: Environmental transformations of galaxies in the SDSS. *Astron. Astrophys.* **2017**, *600*, L6.
191. Järvela, E.; Lähtenmäki, A.; Lietzen, H.; Poudel, A.; Heinämäki, P.; Einasto, M. Large-scale environments of narrow-line Seyfert 1 galaxies. *Astron. Astrophys.* **2017**, *606*, A9.
192. Järvela, E.; Lähtenmäki, A.; Berton, M. Near-infrared morphologies of the host galaxies of narrow-line Seyfert 1 galaxies. *Astron. Astrophys.* **2018**, *619*, A69.

193. Wang, F.; Du, P.; Hu, C.; Bai, J.-M.; Wang, C.-J.; Yi, W.-M.; Wang, J.-G.; Zhang, J.-J.; Xin, Y.-X.; Lun, B.-L.; et al. Reverberation Mapping of the Gamma-Ray Loud Narrow-line Seyfert 1 Galaxy 1H 0323+342. *Astrophys. J.* **2016**, *824*, 149.
194. Czerny, B.; Wang, J.-M.; Du, P.; Hryniewicz, K.; Karas, V.; Li, Y.-R.; Panda, S.; Sniegowska, M.; Wildy, C.; Yuan, Y.-F. Interpretation of Departure from the Broad-line Region Scaling in Active Galactic Nuclei. *Astrophys. J.* **2018**, *870*, 84.
195. Yu, L.-M.; Bian, W.-H.; Wang, C.; Zhao, B.-X.; Ge, X. Calibration of the virial factor  $f$  in supermassive black hole masses of reverberation-mapped AGNs. *Mon. Notices R. Astron. Soc.* **2019**, *488*, 1519.
196. Capetti, A.; Balmaverde, B. The host galaxy / AGN connection in nearby early-type galaxies. A new view of the origin of the radio-quiet/radio-loud dichotomy? *Astron. Astrophys.* **2006**, *453*, 27.
197. Morganti, R.; Holt, J.; Tadhunter, C.; Ramos Almeida, C.; Dicken, D.; Inskip, K.; Oosterloo, T.; Tzioumis, T. PKS 1814-637: A powerful radio-loud AGN in a disk galaxy. *Astron. Astrophys.* **2011**, *535*, A97.
198. Singh, V.; Ishwara-Chandra, C.H.; Sievers, J.; Wadadekar, Y.; Hilton, M.; Beelen, A. Discovery of rare double-lobe radio galaxies hosted in spiral galaxies. *Mon. Notices R. Astron. Soc.* **2015**, *454*, 1556.
199. Abdollahi, S.; Ackermann, M.; Ajello, M.; Albert, A.; Baldini, L.; Ballet, J.; Barbiellini, G.; Bastieri, D.; Becerra Gonzalez, J.; Bellazzini, R.; et al. The Second Catalog of Flaring Gamma-Ray Sources from the Fermi All-sky Variability Analysis. *Astrophys. J.* **2017**, *846*, 34.
200. Kollmeier, J.A.; Zasowski, G.; Rix, H.-W.; Johns, M.; Anderson, S.F.; Drory, N.; Johnson, J.A.; Pogge, R.W.; Bird, J.C.; Blanc, G.A.; et al. SDSS-V: Pioneering Panoptic Spectroscopy. *arXiv* **2017**, arXiv:1711.03234.
201. Hopkins, P.F.; Hernquist, L.; Cox, T.J.; Di Matteo, T.; Martini, P.; Robertson, B.; Springel, V. Black Holes in Galaxy Mergers: Evolution of Quasars. *Astrophys. J.* **2005**, *630*, 705.



© 2019 by the author. Licensee MDPI, Basel, Switzerland. This article is an open access article distributed under the terms and conditions of the Creative Commons Attribution (CC BY) license (<http://creativecommons.org/licenses/by/4.0/>).

